

AD-A100 976

TEXAS UNIV AT AUSTIN APPLIED RESEARCH LABS
STATISTICAL CHARACTERISTICS OF POWER SPECTRUM ESTIMATES DERIVED--ETC(U)
MAY 81 C S PENROD

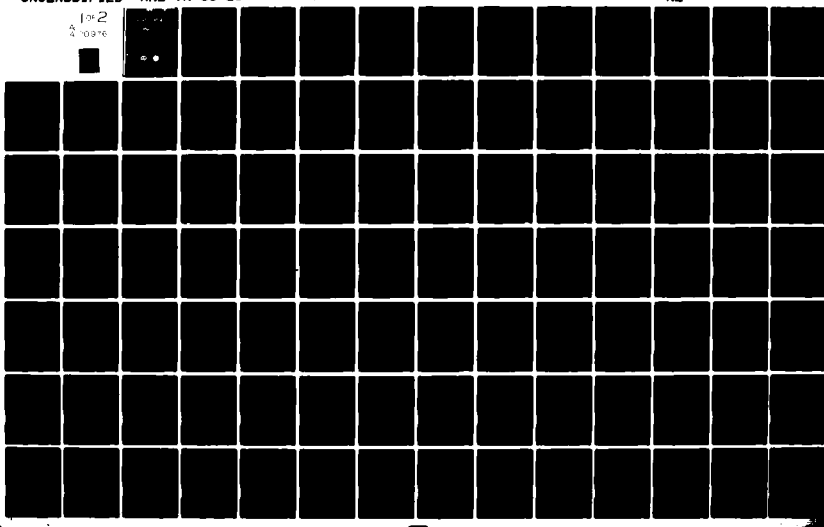
N00039-79-C-0306

NL

UNCLASSIFIED ARL-TR-81-26

F/B 9/4

102
A 0376



AD A100976

AMERICAN

COPY NO. 56

STATISTICAL CHARACTERISTICS OF POWER DIODES
ESTIMATES DERIVED FROM SPARKER DIODE CUTTING TESTS

10 Clark Sponsored

9 Technical rep't.

AUSTIN RESEARCH LABORATORIES
THE UNIVERSITY OF TEXAS AT AUSTIN
POST OFFICE BOX 2680, AUSTIN, TEXAS 78712

11 21 May 81

12 109

Technical Report

APPROVED FOR PUBLIC RELEASE;
DISTRIBUTION UNLIMITED.

13 N00039-79-C-0306

Prepared for:

NAVAL ELECTRONIC SYSTEMS COMMAND
DEPARTMENT OF THE NAVY
WASHINGTON, DC 20380



404434
81 7 02 127 mt

UNCLASSIFIED

SECURITY CLASSIFICATION OF THIS PAGE (When Data Entered)

REPORT DOCUMENTATION PAGE		READ INSTRUCTIONS BEFORE COMPLETING FORM
1. REPORT NUMBER	2. GOVT ACCESSION NO.	3. RECIPIENT'S CATALOG NUMBER
		AD-A100 976
4. TITLE (and Subtitle)	5. TYPE OF REPORT & PERIOD COVERED technical report	
STATISTICAL CHARACTERISTICS OF POWER SPECTRUM ESTIMATES DERIVED FROM HIGHER RESOLUTION FFTs		6. PERFORMING ORG. REPORT NUMBER ARL-TR-81-26
7. AUTHOR(s)	8. CONTRACT OR GRANT NUMBER(s) N00039-79-C-0306	
Clark S. Penrod		
9. PERFORMING ORGANIZATION NAME AND ADDRESS Applied Research Laboratories The University of Texas at Austin Austin, Texas 78712	10. PROGRAM ELEMENT, PROJECT, TASK AREA & WORK UNIT NUMBERS	
11. CONTROLLING OFFICE NAME AND ADDRESS Naval Electronic Systems Command Department of the Navy Washington, DC 20360	12. REPORT DATE 21 May 1981	
14. MONITORING AGENCY NAME & ADDRESS (if different from Controlling Office)	13. NUMBER OF PAGES 115	
	15. SECURITY CLASS. (of this report) UNCLASSIFIED	
	15a. DECLASSIFICATION/DOWNGRADING SCHEDULE	
16. DISTRIBUTION STATEMENT (of this Report) Approved for Public Release; Distribution Unlimited.		
17. DISTRIBUTION STATEMENT (of the abstract entered in Block 20, if different from Report)		
18. SUPPLEMENTARY NOTES		
19. KEY WORDS (Continue on reverse side if necessary and identify by block number) spectrum estimation spectrum resolution		
20. ABSTRACT (Continue on reverse side if necessary and identify by block number) This report documents an investigation of the properties of a technique used to reduce the resolution of a power spectrum estimate. The technique investigated is the familiar one in which averaging across frequency is performed on a spectrum estimate to produce an estimate which has less resolution, but improved stability. Results are presented in various areas. Primarily, the statistical nature of a reduced resolution spectrum produced in this way is characterized by the derivation of expressions for		

UNCLASSIFIED

SECURITY CLASSIFICATION OF THIS PAGE(When Data Entered)

20. (Cont'd)

equivalent degrees of freedom. In addition, the associated spectral windows are determined, and examples are shown which illustrate the effect on the spectrum estimate of various uniform and non-uniform weighting schemes in the frequency averaging. Finally, a particular weighting scheme is shown which produces results which closely approximate the lower resolution estimate obtained by conventional means with the Hanning window.

Accession For	
NTIS GRA&I	<input checked="" type="checkbox"/>
DTIC TAB	<input type="checkbox"/>
Unannounced	<input type="checkbox"/>
Justification _____	
By _____	
Distribution/ _____	
Availability Codes	
Dist	Avail and/or Special
A	

UNCLASSIFIED

SECURITY CLASSIFICATION OF THIS PAGE(When Data Entered)

TABLE OF CONTENTS

	<u>Page</u>
ABSTRACT	iii
LIST OF ILLUSTRATIONS	vii
I. INTRODUCTION	1
II. A BASIC REVIEW OF THE STATISTICAL NATURE OF ESTIMATES OF POWER SPECTRA	5
II.1 Discussion	5
II.2 A Basic Estimate of the Spectrum	7
II.3 Smoothing by Averaging	10
II.4 The Use of Data Windows	11
II.5 Equivalent Degrees of Freedom	14
II.6 Summary	15
III. STATISTICAL STABILITY OF LOW RESOLUTION SPECTRA OBTAINED FROM FREQUENCY AVERAGED HIGH RESOLUTION SPECTRA	17
III.1 Discussion	17
III.2 Non-overlapped High Resolution Transforms with the Rectangular Data Window	18
III.3 Non-overlapped High Resolution Transforms with the Hanning Data Window	19
III.4 50% Overlapped High Resolution Transforms	20
III.5 Examples	23

TABLE OF CONTENTS (Cont'd)

	<u>Page</u>
IV. EFFECTS OF FREQUENCY AVERAGING ON NARROWBAND SIGNALS	31
IV.1 Discussion	31
IV.2 Comparison of Spectral Windows	32
IV.3 Comparison of Estimated Spectra	37
IV.4 Signal Excess Comparison	57
IV.5 Summary	62
V. CONCLUSIONS	63
APPENDIX 1	65
APPENDIX 2	71
APPENDIX 3	79
APPENDIX 4	85
APPENDIX 5	95
REFERENCES	109

LIST OF ILLUSTRATIONS

<u>Figure</u>	<u>Title</u>	<u>Page</u>
1	EQUIVALENT DEGREES OF FREEDOM versus WINDOW LENGTH FOR UNIFORM COEFFICIENTS. T=6L	25
2	EQUIVALENT DEGREES OF FREEDOM versus WINDOW LENGTH FOR 2:1 HSQ COEFFICIENTS. T=6L	26
3	EQUIVALENT DEGREES OF FREEDOM versus WINDOW LENGTH FOR 4:1 HSQ COEFFICIENTS. T=6L	27
4	EQUIVALENT DEGREES OF FREEDOM versus WINDOW LENGTH FOR 8:1 HSQ COEFFICIENTS. T=6L	28
5	SPECTRAL WINDOW COMPARISONS, 2:1 REDUCTION	34
6	SPECTRAL WINDOW COMPARISONS, 4:1 REDUCTION	35
7	SPECTRAL WINDOW COMPARISONS, 8:1 REDUCTION	36
8	COMPARISON OF POWER SPECTRA, 2:1 REDUCTION, L*F=32.000	38
9	COMPARISON OF POWER SPECTRA, 2:1 REDUCTION, L*F=32.100	39
10	COMPARISON OF POWER SPECTRA, 2:1 REDUCTION, L*F=32.200	40
11	COMPARISON OF POWER SPECTRA, 2:1 REDUCTION, L*F=32.300	41
12	COMPARISON OF POWER SPECTRA, 2:1 REDUCTION, L*F=32.400	42
13	COMPARISON OF POWER SPECTRA, 2:1 REDUCTION, L*F=32.500	43
14	COMPARISON OF POWER SPECTRA, 4:1 REDUCTION, L*F=32.000	44
15	COMPARISON OF POWER SPECTRA, 4:1 REDUCTION, L*F=32.100	45
16	COMPARISON OF POWER SPECTRA, 4:1 REDUCTION, L*F=32.200	46
17	COMPARISON OF POWER SPECTRA, 4:1 REDUCTION, L*F=32.300	47
18	COMPARISON OF POWER SPECTRA, 4:1 REDUCTION, L*F=32.400	48
19	COMPARISON OF POWER SPECTRA, 4:1 REDUCTION, L*F=32.500	49
20	COMPARISON OF POWER SPECTRA, 8:1 REDUCTION, L*F=32.000	50
21	COMPARISON OF POWER SPECTRA, 8:1 REDUCTION, L*F=32.100	51

LIST OF ILLUSTRATIONS (Cont'd)

<u>Figure</u>	<u>Title</u>	<u>Page</u>
22	COMPARISON OF POWER SPECTRA, 8:1 REDUCTION, $L^*F=32.200$	52
23	COMPARISON OF POWER SPECTRA, 8:1 REDUCTION, $L^*F=32.300$	53
24	COMPARISON OF POWER SPECTRA, 8:1 REDUCTION, $L^*F=32.400$	54
25	COMPARISON OF POWER SPECTRA, 8:1 REDUCTION, $L^*F=32.500$	55
26	COMPARISON OF NORMALIZED SIGNAL EXCESS, 2:1 REDUCTION	58
27	COMPARISON OF NORMALIZED SIGNAL EXCESS, 4:1 REDUCTION	59
28	COMPARISON OF NORMALIZED SIGNAL EXCESS, 8:1 REDUCTION	60
29	COMPARISON OF POWER SPECTRA, 4:1 REDUCTION, $L^*F=32.000$	98
30	COMPARISON OF POWER SPECTRA, 4:1 REDUCTION, $L^*F=32.100$	99
31	COMPARISON OF POWER SPECTRA, 4:1 REDUCTION, $L^*F=32.200$	100
32	COMPARISON OF POWER SPECTRA, 4:1 REDUCTION, $L^*F=32.300$	101
33	COMPARISON OF POWER SPECTRA, 4:1 REDUCTION, $L^*F=32.400$	102
34	COMPARISON OF POWER SPECTRA, 4:1 REDUCTION, $L^*F=32.500$	103
35	SPECTRAL WINDOW COMPARISONS, 2:1 REDUCTION	104
36	SPECTRAL WINDOW COMPARISONS, 4:1 REDUCTION	105
37	SPECTRAL WINDOW COMPARISONS, 8:1 REDUCTION	106

I. INTRODUCTION

Perhaps the most intuitive, and certainly one of the most useful characterizations of a random process is its power spectrum. Unfortunately, the power spectrum is also a somewhat elusive function in the sense that it cannot be determined unambiguously by observing a process over a finite time interval. So, the problem of how best to use available observations of the process to estimate its spectrum is one which has been of considerable interest to scientists and engineers for many years.

Basic aspects of the spectral analysis problem will be briefly reviewed in this report, but the primary interest here will be on statistical questions revolving around the resolution of a spectrum estimate. It is generally known that, no matter what spectrum estimation technique is used, a decision must be made concerning the trade off between the resolution of the estimate and its stability, or variance. The cost of increased stability is a loss in resolution, or vice versa. It is the possibility of taking advantage of the improved stability of the lower resolution spectrum estimate which makes it desirable to have a method of extracting a lower resolution estimate directly from a high resolution estimate. The ability to reduce resolution quickly and efficiently could make it possible to do frequency domain signal processing at different bandwidths without the expense of reprocessing the original time series. (In many cases the original time series is neither available nor recoverable for reprocessing.) An example of a situation in which this capability could prove useful is one in which signal spectra of various widths are to be detected in the presence of noise. In this case it would generally be

desirable to process the data originally with resolution comparable to the bandwidth of the narrowest line to be detected. Then, in order to enhance the detection capability for broader lines, the original high resolution spectrum could be altered to reduce its resolution and improve its stability. Using the techniques considered in this report, this could be done at much less computational expense than reprocessing the original time series. These techniques could also find application in the conversion of standard fixed resolution spectra to variable resolution where, for example, resolution decreases with increasing frequency.

The frequency averaging techniques to be examined here are not new, and the author is aware of several instances where they have been employed. In brief, they consist of the following procedure. If the resolution of the spectrum is to be reduced by a factor of four, for example, a number of high resolution spectrum values centered around the frequency of the desired low resolution value are averaged together. This is done for each low resolution spectral point desired. In the procedures to be examined here, the number of high resolution points combined to form a low resolution point is allowed to vary, and in some cases the averaging is done with unequal weighting of the high resolution values.

In spite of their widespread usage, no detailed systematic examination of the simulated low resolution spectra produced by these techniques has been published. This report will make several comparisons between the simulated low resolution spectra and conventionally derived low resolution spectra. In particular, the questions to be addressed are:

- (1) What are the statistical characteristics of a simulated low resolution spectrum estimate for a white noise process, and how do they compare with a conventional spectrum estimate which uses the same amount of data?
- (2) When the time series contains a narrowband signal embedded in white noise, how do the simulated and conventional spectra compare when both are derived from the same time series?
- (3) How do the simulated and conventional spectra differ in terms of minimum detectable signal level?
- (4) How does nonuniform weighting of the high resolution values in the frequency averaging affect the comparison in questions 1-3? What weighting functions yield superior performance?

Question (1) is addressed analytically in Chapter III where expressions for the number of equivalent degrees of freedom for the simulated spectra are presented for the case of white Gaussian noise. These expressions are obtained for various direct spectrum estimation techniques including non-overlapped and 50% overlapped, averaged power spectra derived from discrete transformed time series, windowed with various data windows including the Hanning window. With some slight modification the techniques used in the derivations can be extended to other amounts of overlap and to other data windows. However, the cases examined here are representative of techniques currently being employed in practical situations.

Questions (2) through (4) are not readily answered analytically since they are heavily data dependent. Instead, an empirical study via computer simulation is employed, and the results are presented in Chapter IV.

The results demonstrate that the weighting function used in averaging the high resolution values has a significant effect on the simulated low resolution spectrum. A procedure which yielded consistently good results is given for choosing the weighting coefficients. These coefficients produce simulated spectra whose response to narrow band signals is approximately the same as the conventional spectra, and which have approximately the same stability (as measured by equivalent degrees of freedom) as the conventional spectra.

Of the remaining chapters, Chapter V contains a brief summary, while Chapter II is an introduction to, or a basic review of, spectrum estimation. The classic reference for this material is Blackman and Tukey [1]; however, the text by Jenkins and Watts [2] gives a more modern and detailed treatment.

II. A BASIC REVIEW OF THE STATISTICAL NATURE OF ESTIMATES OF POWER SPECTRA

II.1 Discussion

This chapter will serve as a brief review of some of the basic statistical facts associated with the estimation of power spectra from random data. It is not intended to be complete in any sense; however, it should orient the reader to the notation and viewpoint to be used in the remainder of the report. An excellent discussion of the entire subject is contained in Jenkins and Watts [2].

This report will be concerned with the performance of spectrum estimates when the available data $x(t)$ consists of either a sample function taken from a stationary white Gaussian noise process, or such a sample function to which a sinusoid has been added. The stationary random process has an autocovariance function $c_x(\tau)$ defined by

$$c_x(\tau) = E \left\{ [x(t) - m_x][x(t+\tau) - m_x] \right\} , \quad (2.1)$$

where

$$m_x = E \left\{ x(t) \right\} . \quad (2.2)$$

The autocovariance function serves as a useful description of the process although it is not generally a complete description since it involves only second order moments. (It is a complete description, however, when the process is Gaussian.) A more widely used and somewhat more intuitively appealing characterization is the Fourier transform of the autocovariance function, or the power spectral density $S_x(f)$ of the

process. It is the function $S_x(f)$ which we are interested in estimating, basing our estimate on an observation of a single realization of the random process over a time interval of length T .

There are two basic approaches to forming estimates of $S_x(f)$. Until recent years, the more widely used technique consisted of using the observed $x(t)$ to estimate $c_x(\tau)$ for discrete values of τ , and then performing a discrete Fourier transform of the estimate of $c_x(\tau)$ to produce an estimate of $S_x(f)$. This is known as the indirect method, and a wide variety of techniques for implementing it have been discussed in the literature. More recently, with the advent of the FFT (fast Fourier transform) algorithm and faster computers, the preferred technique has become the direct method wherein $x(t)$ itself is sampled and discrete transformed to the frequency domain where its average power, or mean square value, can be resolved into frequency components. The direct method is the one with which we will be concerned.

As with the indirect method, the literature contains a wide range of techniques for implementing the direct method. With each of these techniques the objective is to use the available data to produce an estimate of the spectrum which has small bias, small variance, and the desired resolution. The bias of an estimate is its average error, the variance is a measure of the fluctuation of the estimate around its mean value, and the resolution of the estimate is determined by its ability to resolve spectrum components which are close together in frequency. Designing a spectrum estimator generally involves deciding on trade-offs between these three quantities, since it is usually possible to improve one at the expense of the others. We will be

primarily interested in the trade-off between variance and resolution.

An example of how this trade-off occurs can be seen in a technique which is being used quite extensively to estimate spectra. In this technique the total data length T is broken up into shorter segments of length L which may or may not overlap each other (50% overlap is used commonly). The resulting segments are then sampled, transformed via the FFT, and a power spectrum estimate is obtained for each segment. These estimates are then averaged to form the final estimate. Variance reduction occurs because of the averaging; however, by segmenting the data and doing shorter transforms, we have decreased the resolution capability of the estimate.

In the remaining sections of this chapter various examples of spectrum estimation will be discussed in somewhat more detail. A basic knowledge of probability and statistics is assumed.

II.2 A Basic Estimate of the Spectrum

Let the discrete time (sampled) version of $x(t)$ be denoted

$$x_k = x(k\Delta), \quad 1 \leq k \leq L, \quad (2.3)$$

where

$$\Delta = 1/f_s \quad (2.4)$$

is the time interval between samples. Also, let

$$A_j = \frac{1}{L} \sum_{k=1}^L x_k \cos(2\pi jk/L), \quad (2.5a)$$

$$B_j = \frac{1}{L} \sum_{k=1}^L x_k \sin(2\pi jk/L), \quad (2.5b)$$

$$X_j = A_j + iB_j , \quad i = \sqrt{-1} \quad (2.5c)$$

so that $\{X_j\}$ is the discrete Fourier transform of the sequence $\{x_k\}$.

The sample spectrum based on x_k , $1 \leq k \leq L$, is generally defined as

$$C_x(f_j) = L\Delta |X_j|^2 , \quad (2.6)$$

where

$$f_j = (j-1)/L\Delta . \quad (2.7)$$

It can be shown [2] that under certain conditions $C_x(f_j)$ is an estimate of $S_x(f_j)$ in the sense that

$$\lim_{L\Delta \rightarrow \infty} E\{C_x(f_j)\} = S_x(f_j) . \quad (2.8)$$

However $C_x(f_j)$ is not in itself a good estimate because it does not converge in any statistical sense to $S_x(f_j)$ as the record length L tends to infinity. To illustrate this, we can examine the behavior of the sample spectrum for the case where the x_k are independent identically distributed zero mean Gaussian random variables (e.g., x_k is a discrete white Gaussian noise process). Referring to Eq. (2.5) we see that A_j and B_j are linear combinations of Gaussian random variables, and so A_j and B_j are themselves Gaussian. In fact, if x_k is real Gaussian with mean zero and variance σ^2 (i.e., $x_k \sim N(0, \sigma^2)$), then

$$A_j, B_j \sim N(0, \frac{\sigma^2}{L}) , \quad j = 1, \frac{L}{2} \quad (2.9a)$$

$$A_j, B_j \sim N(0, \frac{\sigma^2}{2L}) , \quad 1 < j < \frac{L}{2} , \quad (2.9b)$$

with the appropriate symmetry for values of j greater than $\frac{L}{2}$. So, for $1 < j < \frac{L}{2}$, we have

$$\begin{aligned} C_x(f_j) &= L\Delta(A_j^2 + B_j^2) \\ &= L\Delta\left[\frac{\sigma^2}{2L}(A_j^2 + B_j^2)\right] \end{aligned} \quad (2.10)$$

where A_j^2 and B_j^2 are $N(0,1)$. The distribution of the sums of the squares of two $N(0,1)$ random variables is well known to be the Chi-square distribution with two degrees of freedom. Hence, for $1 < j < \frac{L}{2}$,

$$C_x(f_j) \sim \frac{\sigma^2\Delta}{2} \chi_2^2 \quad . \quad (2.11)$$

The mean of a Chi-square random variable with v degrees of freedom is simply v , while its variance is $2v$, so for $1 < j < \frac{L}{2}$, the mean of our estimate $C_x(f_j)$ is

$$E\{C_x(f_j)\} = \sigma^2\Delta \quad (2.12)$$

and

$$\text{Var}\{C_x(f_j)\} = \sigma^4\Delta^2 \quad . \quad (2.13)$$

Note that the distribution of $C_x(f_j)$ does not depend on L , the amount of data processed. This result is not surprising when we realize that in this case where L is the transform length, increasing L increases our information about the spectrum, but it also increases the number of frequencies over which the information is spread. The result is no net gain in information at any one frequency, hence the variance remains constant.

II.3 Smoothing by Averaging

Suppose now that we have a data record of length T sec and we wish to produce an estimate with variance somewhat smaller than that of the unsmoothed estimate in the preceding section. This can be accomplished by segmenting the data into P separate pieces (no overlap), each of length $L\Delta$. We can then form estimates $C_x^P(f_j)$, $1 \leq p \leq P$, in the manner described above, where each C_x^P depends on a different segment of the data. The smoothed estimate is then the average, or

$$\bar{C}_x(f_j) = \frac{1}{P} \sum_{p=1}^P C_x^P(f_j) . \quad (2.14)$$

The distribution of \bar{C}_x is easily obtained from the fact that the sum of independent Chi-square random variables has a Chi-square distribution whose number of degrees of freedom is the sum of the degrees of freedom of the component random variables. Hence

$$\bar{C}_x(f_j) \sim \frac{\sigma_\Delta^2}{2P} \chi_{2P}^2 , \quad (2.15)$$

with mean σ_Δ^2 and variance σ_Δ^4/P . We have reduced the variance by a factor $1/P$ simply by limiting the resolution to P times what it would have been had we used a single transform.

The analysis shown here is for the simplest type of smoothed spectral estimate. The use of overlapped transforms and data windows other than the simple rectangular one used here can result in greater variance reduction, but the statistical analysis can become complex.

II.4 The Use of Data Windows

The data window implied in the above analysis is known as the rectangular window in which each L point FFT is performed on an unmodified segment of data. This is equivalent to multiplying the whole data record by a window function which is equal to unity for the segment to be transformed, and zero elsewhere. The resulting transform is then the convolution of the desired transform with the transform of the window function, which in this case is a sinc function (with a phase factor). Therein lies the chief drawback of the rectangular data window. The sidelobes of the sinc function are large, implying that, for spectrum components whose period is not an integral divisor of $L\Delta$, there can be significant "leakage" or spreading of energy into adjacent frequencies. The leakage problem can be reduced by using another data window whose transform has smaller sidelobes, such as the Hanning or cosine window (see Appendix I). The window can be applied in the time domain by multiplying each data value by the appropriate window value before performing the FFT. One advantage of the Hanning window, however, is that it can also be applied quite efficiently in the frequency domain via a three point convolution.

It is interesting to consider the effect of the Hanning window on the variance of an averaged spectrum estimate such as the one discussed in Section II.3. As is pointed out in Appendix I, the window can be applied by convolving the complex coefficients resulting from the FFT of the rectangular windowed time sequence with the sequence

$$W(k) = \begin{cases} 0.5 & , k = 0 \\ -0.25 & , k = \pm 1 \\ 0 & , |k| > 1 \end{cases} . \quad (2.16)$$

If we allow $A_{h,j}$ and $B_{h,j}$ to denote the real and imaginary parts of the Hanned complex coefficients, and let A_j and B_j be as defined in Eq. (2.5), then

$$A_{h,j} = -0.25 A_{j-1} + 0.5 A_j - 0.25 A_{j+1} \quad (2.17a)$$

$$B_{h,j} = -0.25 B_{j-1} + 0.5 B_j - 0.25 B_{j+1} . \quad (2.17b)$$

Again allowing the sequence x_k to be a realization of a discrete white Gaussian noise process, we can easily show that for $2 < j < \frac{L}{2} - 2$,

$$A_{h,j} \sim N(0, 0.375 \frac{\sigma^2}{2L}) , \quad (2.18a)$$

$$B_{h,j} \sim N(0, 0.375 \frac{\sigma^2}{2L}) . \quad (2.18b)$$

Then the distribution of the spectral estimate obtained by averaging P independent Hanned transforms can be obtained using the same techniques used previously:

$$\hat{C}_x(f_j) \sim 0.375 \frac{\sigma^2}{2P} x_{2P}^2 . \quad (2.19)$$

We see that for the white Gaussian noise case, $\hat{C}_x(f_j)$ is essentially the same random variable as $\bar{C}_x(f_j)$, multiplied by a constant scale factor. (Alternatively, we could note that $\bar{C}_x(f_j)$ and $\hat{C}_x(f_j)$ have the same number of equivalent degrees of freedom.) So, although the Hanning window does

reduce the leakage problem, it actually does not contribute to estimate stability in the case of averaged non-overlapped transforms.

As a final comment on the use of the Hanning window, we would like to point out its effect on the frequency autocovariance of the spectrum estimate. The autocovariance function is derived in Appendix 3 and will only be stated here. Let C'_x be a spectrum estimate resulting from a single Hanned transform. Then, for $2 < i, j < \frac{N}{2} - 2$,

$$\text{Cov}\left\{C'_x(f_i), C'_x(f_j)\right\} = \begin{cases} 1.406 \times 10^{-1} \sigma^4 \Delta^4, & |i-j| = 0 \\ 6.250 \times 10^{-2} \sigma^4 \Delta^2, & |i-j| = 1 \\ 3.907 \times 10^{-3} \sigma^4 \Delta^2, & |i-j| = 2 \\ 0. & |i-j| \geq 3 \end{cases} . \quad (2.20)$$

For P non-overlapped Hanned transforms,

$$\text{Cov}\left\{\bar{C}'_x(f_i), \bar{C}'_x(f_j)\right\} = \frac{1}{P} \text{Cov}\left\{C'_x(f_i), C'_x(f_j)\right\} . \quad (2.21)$$

From Eq. (2.21) we see that averaging several non-overlapped Hanned spectra has no real effect on frequency autocovariance since normalization of the resulting functions yields the same normalized autocovariance for both. For comparison purposes we note that when the rectangular data window is used in the white Gaussian noise case, the Fourier coefficients are independent resulting in

$$\text{Cov}\left\{\bar{C}'_x(f_i), \bar{C}'_x(f_j)\right\} = \begin{cases} \frac{\sigma^4 \Delta^2}{P}, & i = j \\ 0, & i \neq j \end{cases} . \quad (2.22)$$

We can conclude that although leakage is reduced, which is important when narrow band signals are present in the data, we have introduced some correlation in the noise portion of the spectrum by using a window other than the rectangular window.

II.5 Equivalent Degrees of Freedom

There are a number of spectral estimation techniques which yield estimates whose distributions, unlike those discussed above, are not that of a constant times a Chi-square random variable. To compare the stability of these estimates, a common approach is to approximate the perhaps unknown distribution of the spectrum estimate with a distribution which is that of a constant times a Chi-square random variable. The approximation is in terms of first and second order moments. Let X be the random variable whose distribution is to be approximated by that of αY , where Y is Chi-square with v degrees of freedom. We assume that the mean and variance of X can be calculated. Then, in order to determine appropriate values for α and v , we equate means and variances:

$$EX = E\alpha Y = \alpha EY = \alpha v , \quad (2.23)$$

$$\text{Var } X = \text{Var } \alpha Y = \alpha^2 \text{Var } Y = 2\alpha^2 v . \quad (2.24)$$

Solving for α and v yields

$$\alpha = \frac{\text{Var } X}{2EX} , \quad (2.25)$$

$$v = \frac{2E^2 X}{\text{Var } X} . \quad (2.26)$$

Hence, if we can compute the mean and variance of the spectrum estimate, we can compute the number of degrees of freedom of a Chi-square approximation to its distribution. This is termed the number of equivalent degrees of freedom of the estimate. Its value as an indicator of the stability of an estimate lies in the fact that it increases as the size of the variance, relative to the mean, decreases. It should be borne in mind, however, that the Chi-square distribution corresponding to the equivalent degrees of freedom is only an approximation to the true distribution of the spectrum estimate.

II.6 Summary

In this chapter and the appendices referred to, we have tried to present some basic material which is fundamental to the remainder of the report. Both the material presented and the presentation are by no means complete; however the interested reader should be able to satisfy the shortcomings by referring to Jenkins and Watts [2], Bergland [3], Cooley et al. [4], or Richards [5]. These references are only a sampling of a number of papers and texts addressing basic topics related to direct spectrum estimation via the FFT.

III. STATISTICAL STABILITY OF LOW RESOLUTION SPECTRA OBTAINED FROM FREQUENCY AVERAGED HIGH RESOLUTION SPECTRA

III.1 Discussion

The frequency averaging methods by which low resolution spectrum estimates are derived from high resolution estimates are straightforward and intuitively obvious. We simply partition the frequency range into a number of intervals or bands whose widths correspond to the desired frequency resolution for the low resolution estimate. We then perform a weighted average over all the high resolution spectrum values in each band. The procedure can be generalized by allowing the low resolution bands to overlap so that some of the high resolution points may enter into more than one of the weighted averages.

In this chapter we will present formulae which will allow computation of the number of equivalent degrees of freedom of a spectrum obtained by frequency averaging. We will assume that the time series on which the estimates are based is simply a discrete white Gaussian noise process. The derivations have been completed for cases where the high resolution spectrum was estimated using both overlapped and non-overlapped transforms, with rectangular, Hanning, and other data windows. The principal importance of these results is that they allow us to determine weighting coefficients for frequency averaging which will produce a low resolution estimate with the desired stability. For example, in some of the empirical studies to be presented in Chapter IV, the weighting coefficients were chosen to produce a simulated low resolution spectrum with the same number of equivalent degrees of freedom as a conventionally obtained spectrum based on the same amount of data.

The results are grouped in Sections III.2-III.4 according to the method used to produce the high resolution estimate. The derivations are contained in Appendices 2 and 4.

III.2 Non-overlapped High Resolution Transforms with the Rectangular Data Window

Let $C(f_j)$ denote a power spectrum estimate produced by averaging P non-overlapped rectangular windowed transforms, and define the frequency averaged low resolution spectrum derived from C by

$$\hat{C}(f_k) = \sum_{j=-K}^K a_j C(f_{k-j}) \quad . \quad (3.1)$$

The low resolution spectrum estimate for frequency f_j is then a weighted sum of $2K+1$ high resolution spectrum values centered around f_k . The computation of the number of equivalent degrees of freedom v of $\hat{C}(f_k)$ can be carried out easily using Eq. (2.26).

$$v = \frac{2E^2 \hat{C}(f_k)}{\text{Var } \hat{C}(f_k)} \quad (3.2)$$

$$= \frac{2E^2 \left\{ \sum_{j=-K}^K a_j C(f_{k-j}) \right\}}{\text{Var} \left\{ \sum_{j=-K}^K a_j C(f_{k-j}) \right\}} \quad . \quad (3.3)$$

It was pointed out in Chapter II that the random variables $C(f_j)$ are independent over j , so we have

$$v = \frac{2 \left[\sum_{j=-K}^K a_j E\{C(f_{k-j})\} \right]^2}{\sum_{j=-K}^K a_j^2 \text{Var}\{C(f_{k-j})\}} \quad (3.4)$$

Also from Chapter II, we know that for values of j sufficiently removed from the endpoints of the spectrum,

$$E\{C(f_j)\} = \sigma^2 \Delta \quad (3.5)$$

$$\text{Var}\{C(f_j)\} = \sigma^4 \Delta^2 / P \quad (3.6)$$

Hence,

$$v = \frac{2P \left(\sum_{j=-K}^K a_j \right)^2}{\sum_{j=-K}^K a_j^2} \quad (3.7)$$

III.3 Non-overlapped High Resolution Transforms with the Hanning Data Window

For this case, only the results will be stated and the derivation will be deferred to Appendix 2. Using the same notation used above,

$$v = \frac{0.5625 P \left(\sum_{j=-K}^K a_j \right)^2}{\sum_{k=-K}^K \sum_{j=-K}^K a_k a_j D(k,j) - 0.1406 \left(\sum_{j=-K}^K a_j \right)^2}, \quad (3.8)$$

where

$$D(k,j) = \begin{cases} 0.4219 & , \quad k=j \\ 0.2656 & , \quad |k-j| = 1 \\ 0.1719 & , \quad |k-j| = 2 \\ 0.1406 & , \quad |k-j| \geq 3 \end{cases} . \quad (3.9)$$

In cases where the weighting coefficients a_i are all equal and the frequency averaging includes $N \geq 4$ high resolution spectrum points, Eq. (3.8) reduces to

$$v = \frac{5.63N^2P}{5.47N - 2.81} . \quad (3.10)$$

III.4 50% Overlapped High Resolution Transforms

For this case also, only the results will be stated. The derivation is in Appendix 4. In this case,

$$v = \frac{2PI_o^2 \left(\sum_{j=-K}^K a_j \right)^2}{\sum_{k=-K}^K \sum_{j=-K}^K a_k a_j \left\{ I_1^2(k,j) + \frac{2(P-1)}{P} I_2^2(k,j) \right\}} , \quad (3.11)$$

where

$$(1) \quad I_o = \int_{-\infty}^{\infty} |W(f)|^2 df , \quad (3.12)$$

$$(2) \quad I_1(k,j) = \left| \int_{-\infty}^{\infty} W(f) W^*(f + \delta_{k,j}) df \right| , \quad (3.13)$$

$$(3) \quad I_2(k, j) = \left| \int_{-\infty}^{\infty} W(f) W^*(f + \delta_{k,j}) e^{i\pi L f} df \right| , \quad (3.14)$$

$$(4) \quad \delta_{k,j} = \frac{k - j}{L} , \quad (3.15)$$

(5) P is the number of overlapped high resolution transforms averaged together to form $C(f_j)$, and

(6) $W(f)$ is the spectral window, or the Fourier transform of the data window.

When the Hanning window is used (Appendix 1),

$$W(f) = \frac{L \operatorname{sinc}(Lf)}{2[1-(Lf)^2]} . \quad (3.16)$$

Evaluating the integral in Eq. (3.12) yields, for the Hanning window,

$$I_0 = 0.1406L^2 . \quad (3.17)$$

The integrals in Eqs. (3.13) and (3.14) have been evaluated numerically for the Hanning window:

$$|I_1(k, j)|^2 = \begin{cases} 1.406 \times 10^{-1} L^2 & , \quad k=j \\ 6.250 \times 10^{-2} L^2 & , \quad |k-j| = 1 \\ 3.906 \times 10^{-3} L^2 & , \quad |k-j| = 2 \\ \approx 0 & , \quad |k-j| \geq 3 \end{cases} ; \quad (3.18)$$

$$|I_2(k, j)|^2 = \begin{cases} 3.906 \times 10^{-3} L^2 & , \quad k=j \\ 2.814 \times 10^{-3} L^2 & , \quad |k-j| = 1 \\ 9.766 \times 10^{-4} L^2 & , \quad |k-j| = 2 \\ 1.126 \times 10^{-4} L^2 & , \quad |k-j| = 3 \\ \approx 0 & , \quad |k-j| \geq 4 \end{cases} . \quad (3.19)$$

Substituting these values back into Eq. (3.11), we have for the Hanning window,

$$v = \frac{2.813 \times 10^{-1} P \left(\sum_{j=-K}^K a_j \right)^2}{\sum_{k=0}^3 \left\{ H_k \left[\sum_{\substack{i, j: \\ |i-j|=k}} a_i a_j \right] \right\}} , \quad (3.20)$$

where

$$H_0 = 1.406 \times 10^{-1} + \frac{2(P-1)}{P} (3.906 \times 10^{-3}) , \quad (3.21a)$$

$$H_1 = 6.250 \times 10^{-2} + \frac{2(P-1)}{P} (2.814 \times 10^{-3}) , \quad (3.21b)$$

$$H_2 = 3.906 \times 10^{-3} + \frac{2(P-1)}{P} (9.766 \times 10^{-4}) , \quad (3.21c)$$

$$H_3 = \frac{2(P-1)}{P} (1.126 \times 10^{-4}) . \quad (3.21d)$$

III.5 Examples

In this section we will use the above results to calculate equivalent degrees of freedom for frequency averaged low resolution spectrum estimates. The calculations will be done for two types of weighting coefficients used in the averaging. Since the most commonly used coefficients are uniform (all the coefficients are equal), this case was chosen for one example. In addition, some effort was devoted to finding a method of choosing coefficients which would produce a frequency averaged low resolution spectrum whose characteristics were as similar as possible to those of a conventionally obtained spectrum with the same resolution based on the same data. This resulted in a set of weighting coefficients which will be referred to as the HSQ coefficients, obtained from the following equation:

$$a_j = \frac{\text{sinc}^2(\alpha j)}{(1 - \alpha^2 j^2)^2} . \quad (3.22)$$

Here, α is the ratio of the desired low resolution to the higher resolution from which the frequency averaged spectrum is to be obtained. The coefficients derived from Eq. (3.22) can then be used in Eq. (3.1) for the frequency averaging.

While doing the examples for this report, we were primarily interested in reducing resolution by factors of two, four, and eight, corresponding to α values of 0.5, 0.25, and 0.125, respectively. The example computations are performed for a situation where the high resolution transform length L was one-sixth of the total available data T . Hence P was equal to six if non-overlapped transforms were

used, or eleven if 50% overlapped transforms were used. The results of the calculations are shown in Figs. 1-4 for the four types of weighting coefficients. In each figure are shown three curves corresponding to high resolution processing using non-overlapped transforms with rectangular and Hanning windows, and 50% overlapped transforms with the Hanning window. The number of equivalent degrees of freedom of the frequency averaged spectrum was plotted versus the number of coefficients used. For example, if K were equal to seven in Eq. (3.1), then 15 coefficients would be used. If these coefficients were uniform, and if the high resolution spectrum was derived from non-overlapped Hanned transforms, then, from Fig. 1, the low resolution spectrum would have approximately 95 equivalent degrees of freedom.

The effect of the Hanning window in introducing correlation across frequency into the spectrum appears in each example. This is the reason why the rectangular windowed spectrum, with its absence of frequency correlation, produces more equivalent degrees of freedom per window coefficient than the Hanning windowed spectrum. This is generally true except when overlapped transforms and a small number of coefficients are used. In this case the effect of the increased number of transforms outweighs the effect of frequency correlation resulting in a larger number of equivalent degrees of freedom than produced by non-overlapped transforms with the rectangular window.

For comparison purposes, we point out that from [Ref. 6, Eq. (36)] we can compute the number of equivalent degrees of freedom for the high resolution spectrum when 50% overlapped Hanned transforms are used. The resulting value is approximately 21. A 2:1 reduction

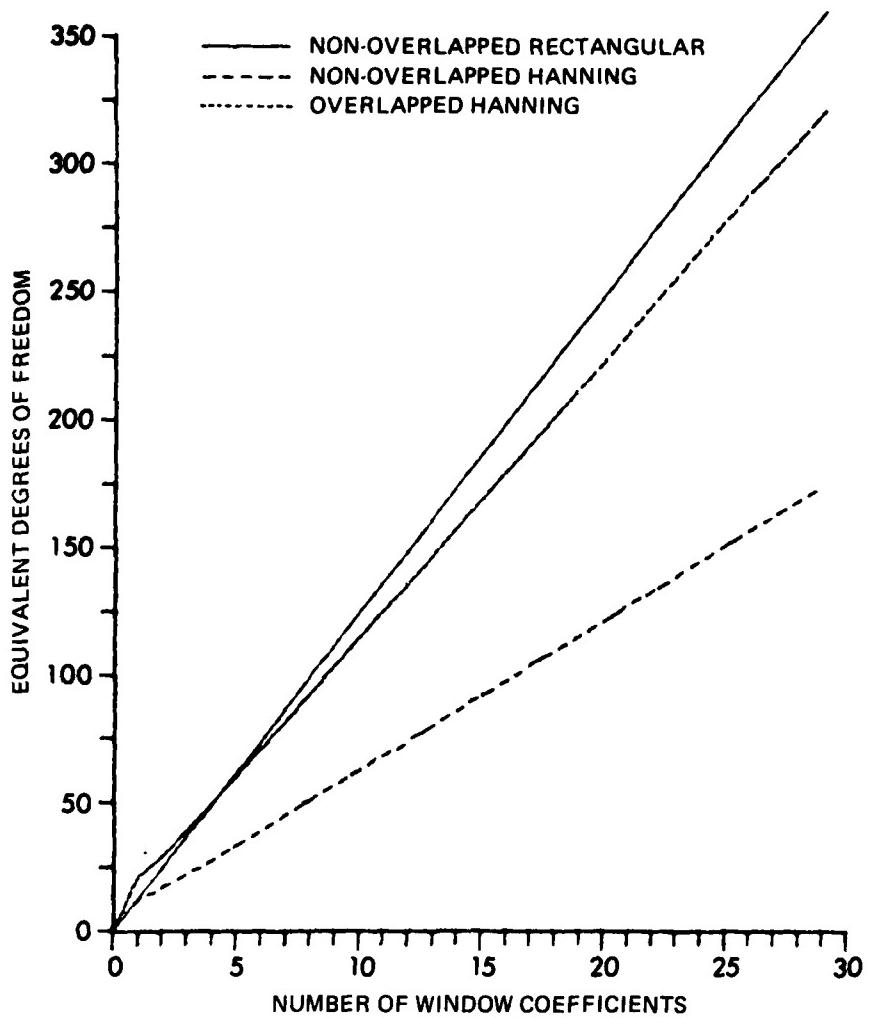


FIGURE 1
EQUIVALENT DEGREES OF FREEDOM versus WINDOW LENGTH
FOR UNIFORM COEFFICIENTS, $T = 6L$

ARL:UT
AS-78-1487
CSP - GA
6-15-81

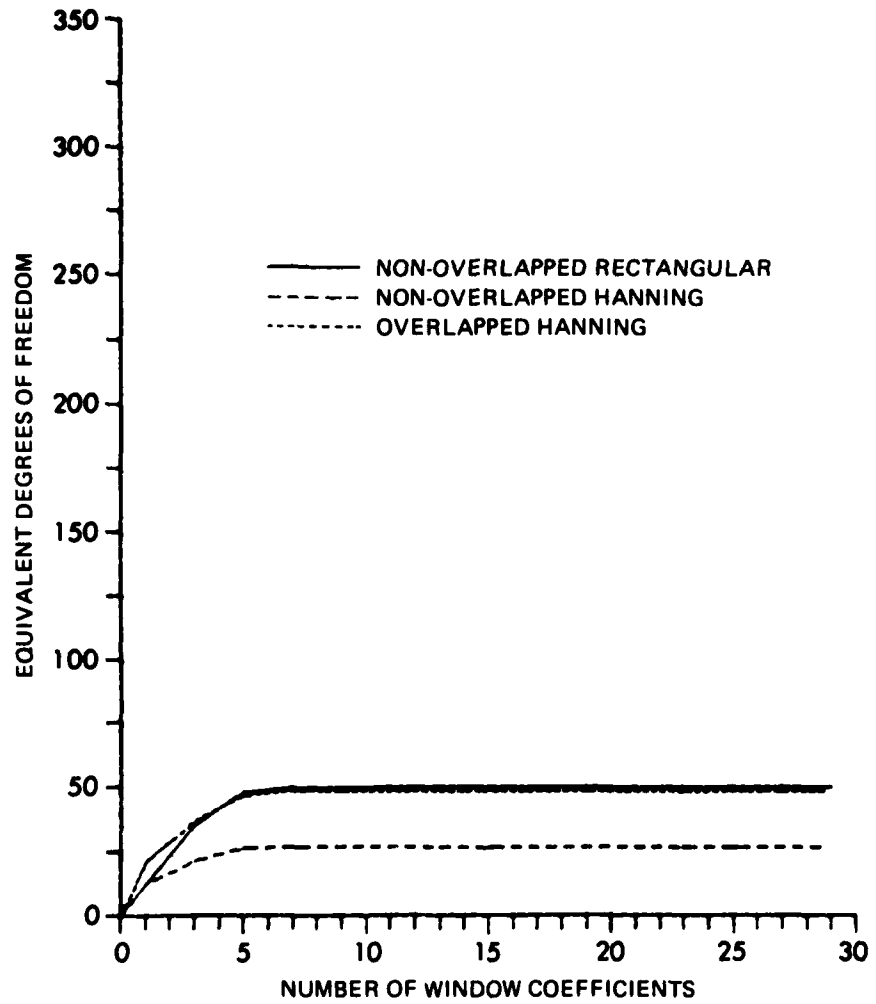


FIGURE 2
EQUIVALENT DEGREES OF FREEDOM versus WINDOW LENGTH
FOR 2:1 HSQ COEFFICIENTS, $T = 6L$

ARL:UT
AS-7B-1488
CSP - GA
6-15-81

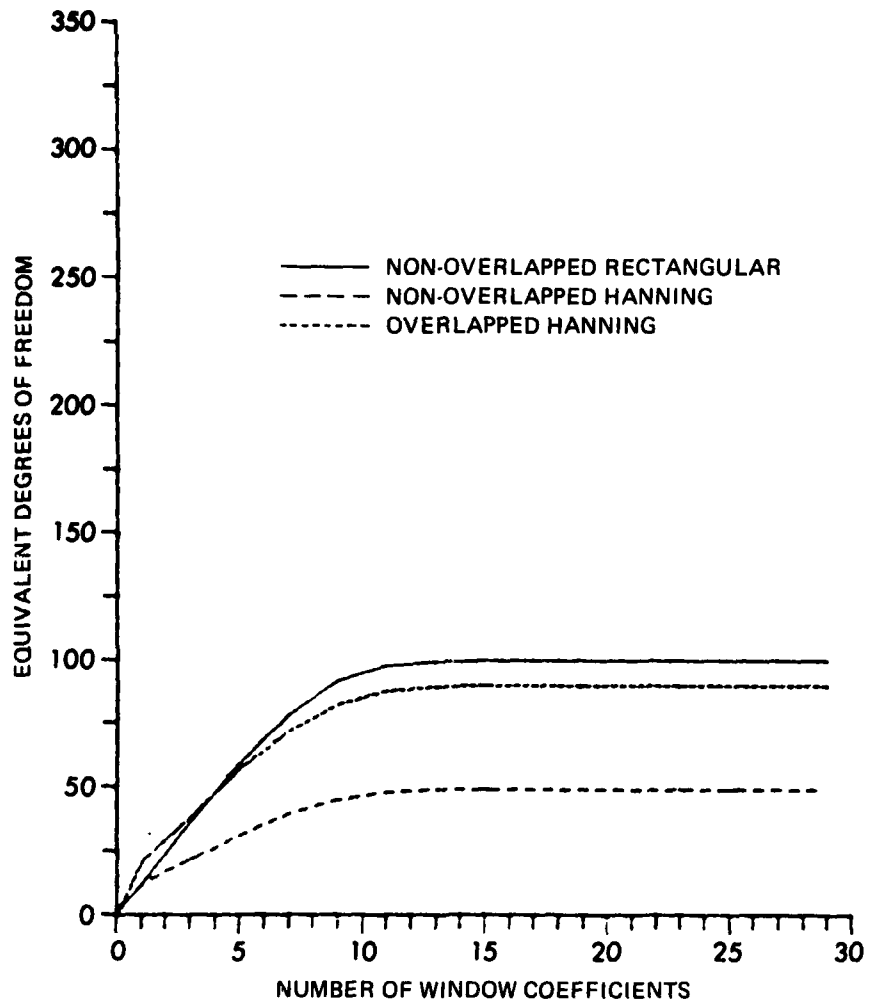


FIGURE 3
EQUIVALENT DEGREES OF FREEDOM versus WINDOW LENGTH
FOR 4:1 HSQ COEFFICIENTS, T = 6L

ARL:UT
AS-78-1489
CSP - GA
6-15-81

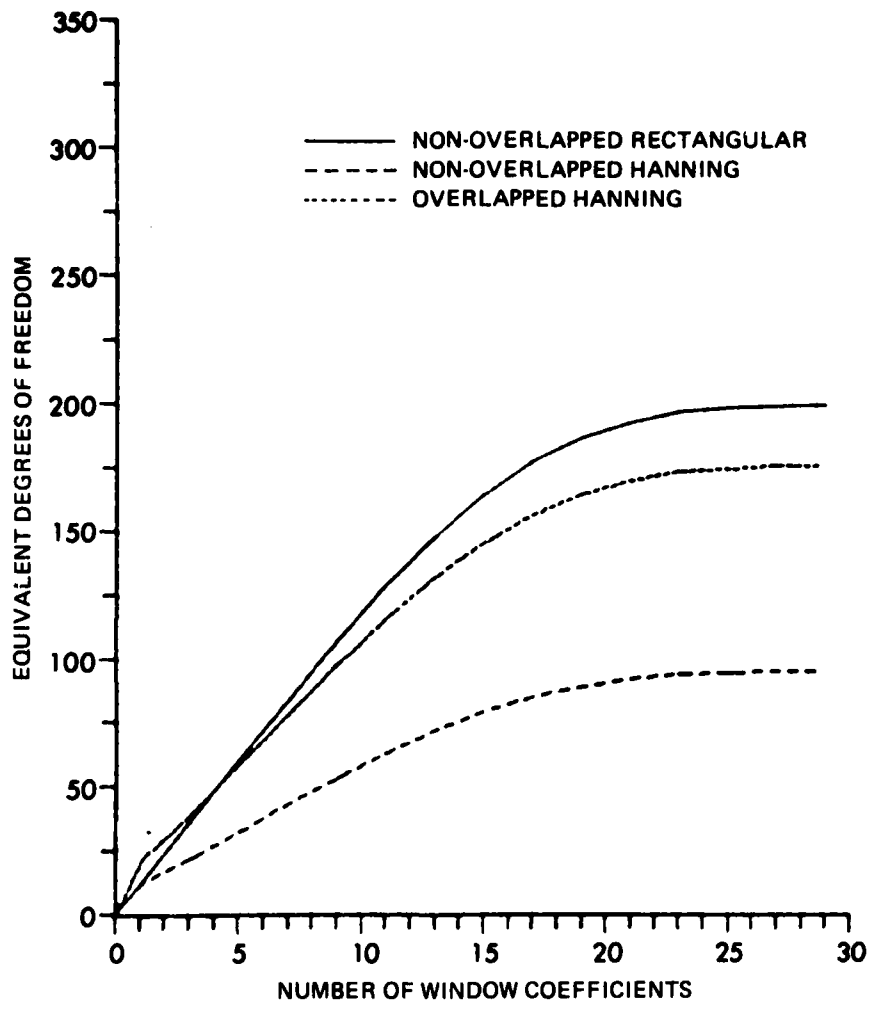


FIGURE 4
EQUIVALENT DEGREES OF FREEDOM versus WINDOW LENGTH
FOR 8:1 HSQ COEFFICIENTS, T = 6L

ARL:UT
AS-78-1490
CSP - GA
6-15-81

in resolution with the same type of processing using shorter transforms and the same amount of data would yield 44 equivalent degrees of freedom, while a 4:1 reduction would yield 89 and an 8:1 reduction would yield 180 equivalent degrees of freedom. For the examples to be presented in the following chapter we will choose a window length which produces approximately the same number of equivalent degrees of freedom as would have been produced by conventional low resolution processing of the same data. In other words, if we were to take the high resolution spectrum in this example and reduce the resolution by frequency averaging instead of reprocessing the data, we would choose a window length based on the graphs of Figs. 1-4 which would yield 44, 89, or 180 equivalent degrees of freedom for 2:1, 4:1, or 8:1 reduction ratios. This would insure that the frequency averaged spectrum would have the same statistical stability as a spectrum produced by reprocessing the original data with shorter transforms.

CHAPTER IV

EFFECTS OF FREQUENCY AVERAGING ON NARROWBAND SIGNALS

IV.1 Discussion

In the preceding chapters, interest has been primarily in the estimation of power spectra for data consisting solely of random noise. In Chapter III, formulae were obtained which would allow determination of the number of equivalent degrees of freedom possessed by a frequency averaged low resolution spectrum as a function of the averaging coefficients. In this chapter, we will be concerned with the performance of the averaging techniques when the data contains a sinusoid in addition to the random noise.

Our objective here is to compare various aspects of the performance of spectrum estimates obtained by frequency averaging with estimates obtained by conventional processing of the data, where the comparisons are made with effects on detection in mind. The comparisons are made by generating a data sequence consisting of a sinusoid plus random noise. Two spectrum estimates are then produced from the same data. One estimate, the conventional one, employs fifty percent overlapped FFTs in the manner described previously. The other estimate, the frequency averaged one, is derived from a higher resolution spectrum which also resulted from fifty percent overlapped FFTs. In all of the examples presented here, the weighting coefficients are chosen to produce a frequency averaged spectrum with approximately the same number of equivalent degrees of freedom as the conventionally

derived spectrum. Examples are presented in which the resolution reduction is by factors of 2:1, 4:1, and 8:1. Spectrum comparisons are made for several sinusoidal signal frequencies evenly spaced between FFT frequencies. The weighting coefficients used are the HSQ and uniform coefficients described in Section III.5. The coefficients used in all the examples in this chapter are shown in Table 4.1.

They are normalized so that their sum is unity.

IV.2 Comparison of Spectral Windows

This section is concerned with the shape of the spectral window associated with frequency averaged spectra. Knowledge of the spectral window, and how it compares with such commonly used windows as the Hanning window, is important since it indicates how much leakage of energy into adjacent frequencies will occur for sinusoids whose period is not an integral divisor of the time length of the FFT.

Spectral windows were determined for signals in the absence of noise for both HSQ and uniform coefficients. They are plotted in Figs. 5-7 along with the Hanning window used in producing the conventional estimate.

A few words of explanation are in order concerning these figures. The abscissa values of frequency are normalized by multiplying the actual signal frequency by the time length of the low resolution transform used in the conventional estimate. Hence integer values of frequency correspond to the discrete frequencies at which the FFT evaluates the transform. Spreading can be determined from the graphs as follows. Suppose we have a signal which is 0.75 normalized frequency units away from an FFT frequency. If the Hanning window is used with conventional processing, it will produce a contribution to the energy

TABLE 4.1
COEFFICIENTS FOR FREQUENCY AVERAGING

	HSQ Coefficients	Uniform Coefficients
2:1 Reduction	$K = 2, EDF = 46.5$ $a_0 = 0.3400$ $a_{\pm 1} = 0.2450$ $a_{\pm 2} = 0.0850$	$K = 1, EDF = 38.4$ $a_0 = 0.3333$ $a_{\pm 1} = 0.3333$ \vdots
4:1 Reduction	$K = 6, EDF = 89.3$ $a_0 = 0.1670$ $a_{\pm 1} = 0.1540$ $a_{\pm 2} = 0.1203$ $a_{\pm 3} = 0.0786$ $a_{\pm 4} = 0.0417$ $a_{\pm 5} = 0.0171$ $a_{\pm 6} = 0.0048$	$K = 4, EDF = 100.5$ $a_0 = 0.1111$ $a_{\pm 1} = 0.1111$ $a_{\pm 2} = 0.1111$ $a_{\pm 3} = 0.1111$ $a_{\pm 4} = 0.1111$
8:1 Reduction	$K = 12, EDF = 174.6$ $a_0 = 0.0836$ $a_{\pm 1} = 0.0819$ $a_{\pm 2} = 0.0771$ $a_{\pm 3} = 0.0696$ $a_{\pm 4} = 0.0602$ $a_{\pm 5} = 0.0498$ $a_{\pm 6} = 0.0393$ $a_{\pm 7} = 0.0295$ $a_{\pm 8} = 0.0209$ $a_{\pm 9} = 0.0139$ $a_{\pm 10} = 0.0086$ $a_{\pm 11} = 0.0048$ $a_{\pm 12} = 0.0024$	$K = 8, EDF = 184.3$ $a_0 = 0.0588$ $a_{\pm 1} = 0.0588$ $a_{\pm 2} = 0.0588$ $a_{\pm 3} = 0.0588$ $a_{\pm 4} = 0.0588$ $a_{\pm 5} = 0.0588$ $a_{\pm 6} = 0.0588$ $a_{\pm 7} = 0.0588$ $a_{\pm 8} = 0.0588$

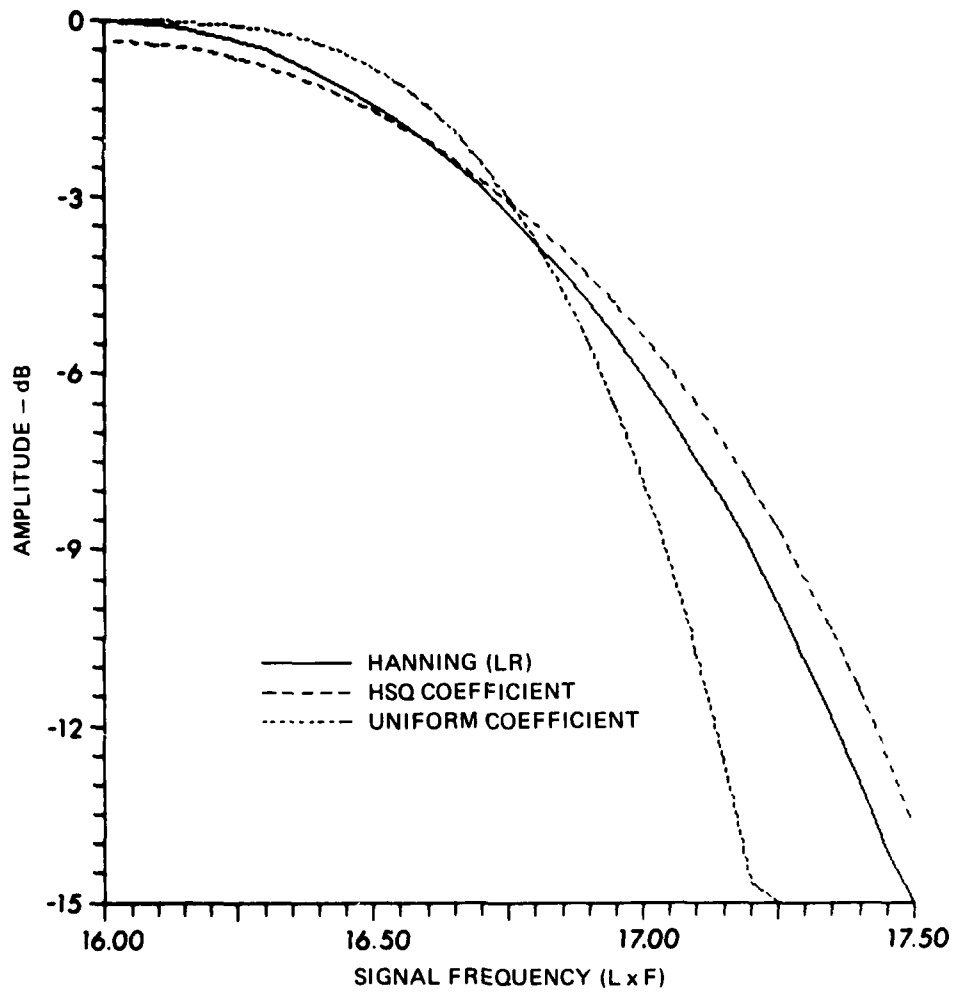


FIGURE 5
SPECTRAL WINDOW COMPARISONS, 2:1 REDUCTION

ARL:UT
AS-78-1491
CSP - GA
6-15-81

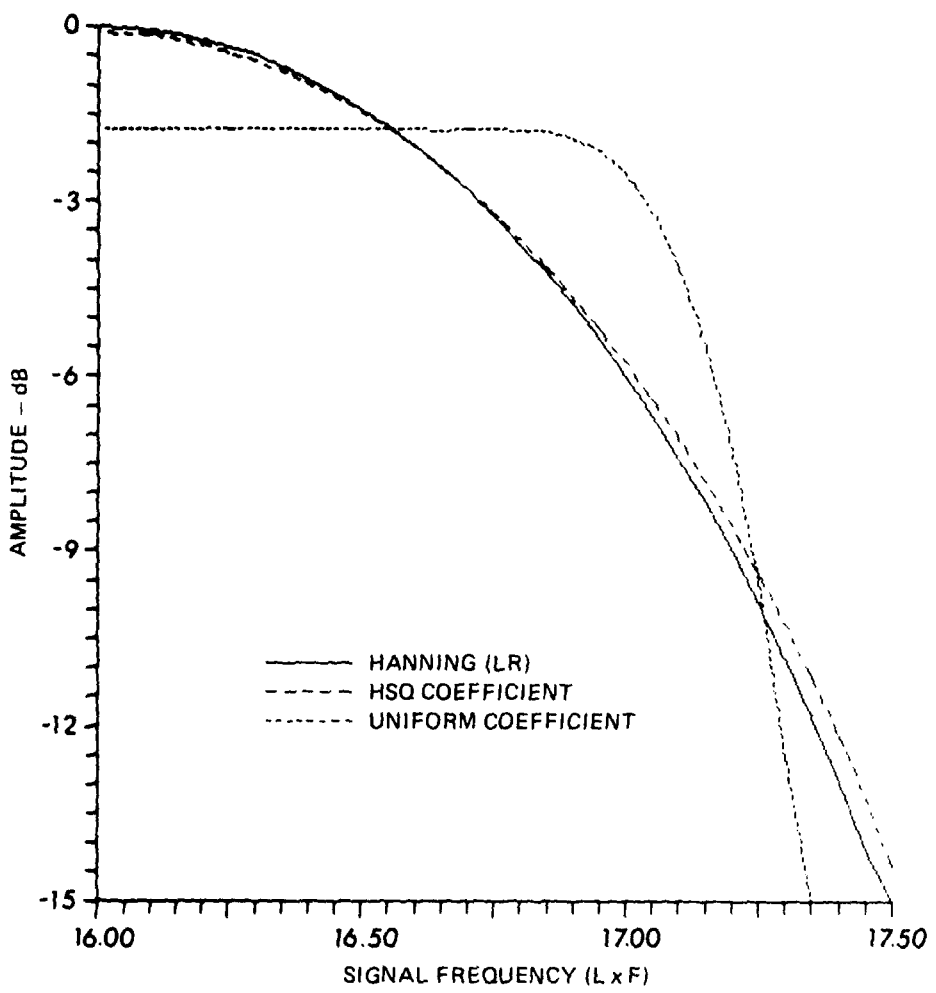


FIGURE 6
SPECTRAL WINDOW COMPARISONS, 4:1 REDUCTION

ARL:UT
AS-78-1492
CSF - GA
6-15-81

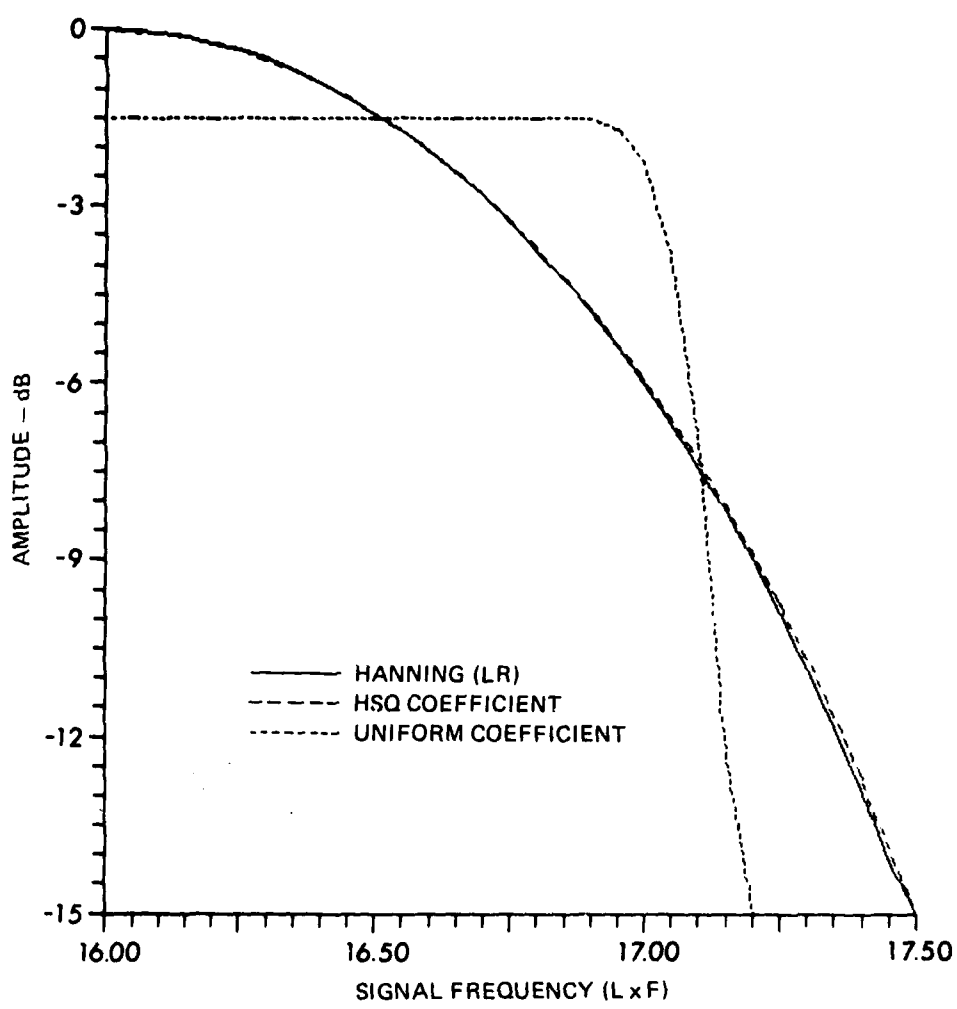


FIGURE 7
SPECTRAL WINDOW COMPARISONS, 8:1 REDUCTION

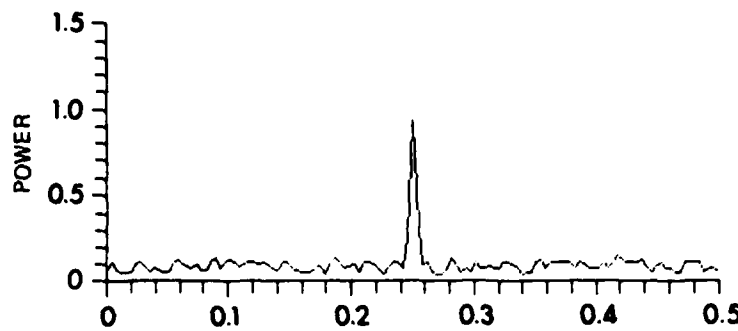
ARL:UT
AS-78-1493
CSP - GA
6-15-81

at that FFT frequency which is 3.4 dB less than its contribution would have been had its frequency been the same as the FFT frequency.

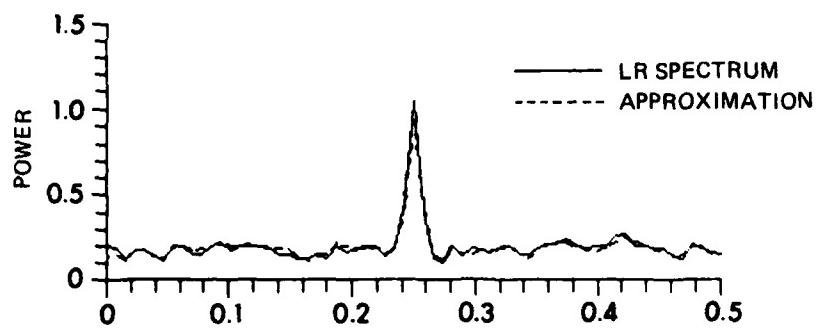
The graphs reveal that HSQ coefficients, matched to conventional processing in equivalent degrees of freedom, also produce a spectral window which matches the Hanning window quite closely. The graphs also reveal that when enough uniform coefficients are used to produce the required number of equivalent degrees of freedom, the resulting spectral window is somewhat broader resulting in less resolution capability. Resolution can be restored by using fewer coefficients, but this will be at the cost of spectrum stability in terms of equivalent degrees of freedom. Finally, the graphs show that the spectral window can be tailored significantly by varying the coefficients used in the frequency averaging.

IV.3 Comparison of Estimated Spectra

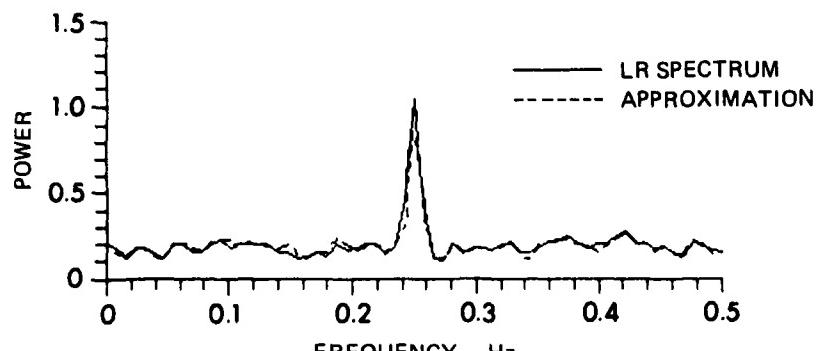
Figures 8-25 are plots of various estimates of the power spectrum of a sinusoid in the presence of noise. A few words of explanation are in order concerning these plots. A 1 Hz sampling rate was used, so the spectra are shown from DC to the Nyquist frequency of 0.5 Hz. The sinusoid (signal) frequency is given in the title of each plot in normalized frequency units, i.e., the true frequency is multiplied by the length of a low resolution (short) transform. In each of these examples, the low resolution transform length was chosen to be 128 points, while the high resolution transforms were 256, 512, or 1024 points for 2:1, 4:1, and 8:1 reductions in resolution. Using the normalized frequency units, integer values of signal frequency correspond to FFT frequencies. Since the response of the spectrum estimates to sinusoids



HIGH RESOLUTION SPECTRUM



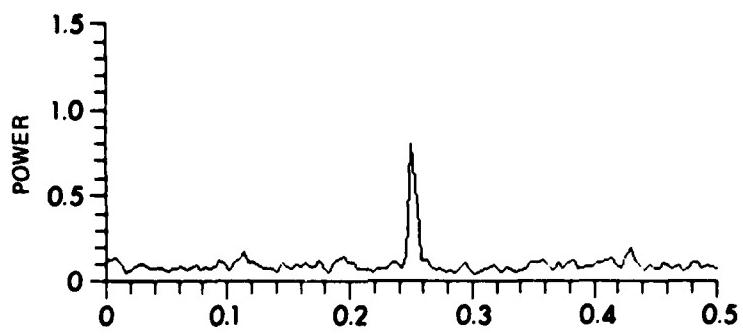
APPROXIMATION OF LR SPECTRUM WITH HSQ COEFFICIENT



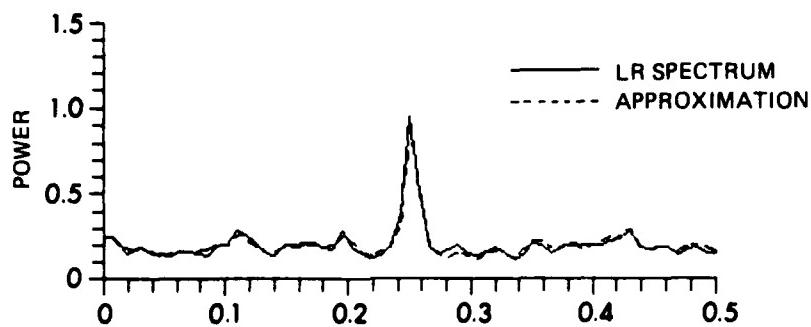
APPROXIMATION OF LR SPECTRUM WITH UNIFORM COEFFICIENT

FIGURE 8
COMPARISON OF POWER SPECTRA
2:1 REDUCTION, $L \times F = 32.000$

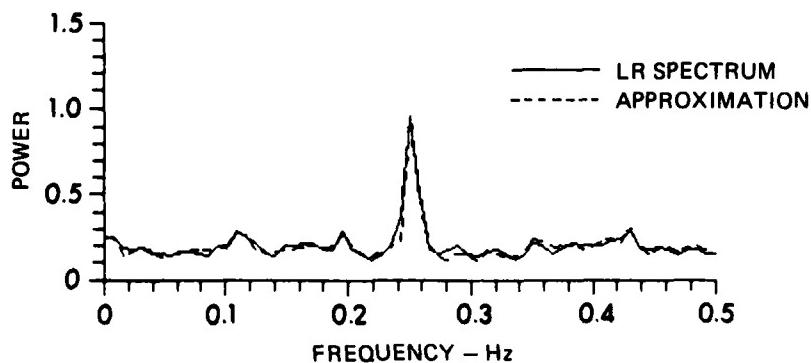
ARL:UT
AS-78-1494
CSP - GA
6-15-81



HIGH RESOLUTION SPECTRUM



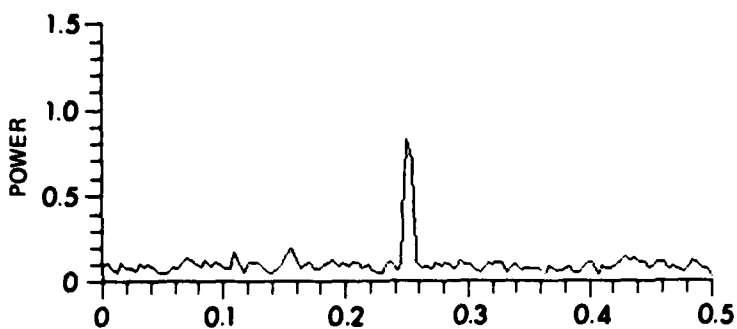
APPROXIMATION OF LR SPECTRUM WITH HSQ COEFFICIENT



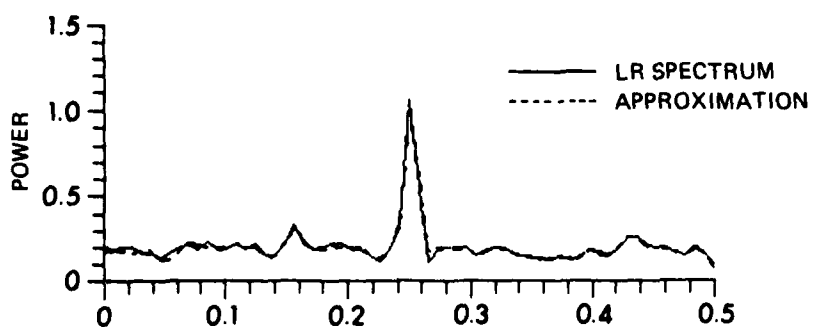
APPROXIMATION OF LR SPECTRUM WITH UNIFORM COEFFICIENT

FIGURE 9
COMPARISON OF POWER SPECTRA
2:1 REDUCTION, $L \times F = 32.100$

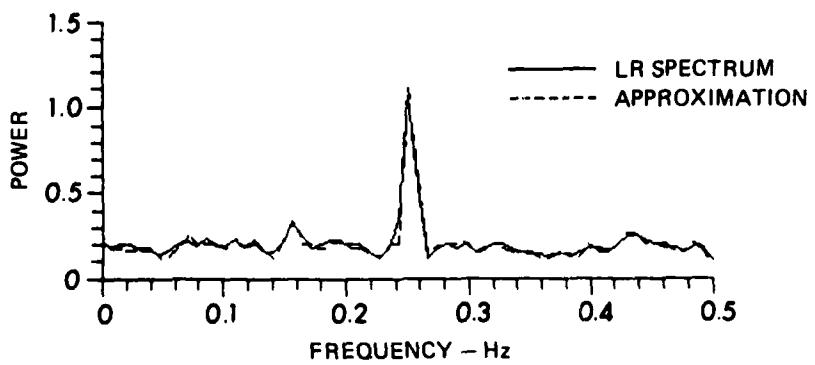
ARL:UT
AS-78-1495
CSP - GA
6-15-81



HIGH RESOLUTION SPECTRUM



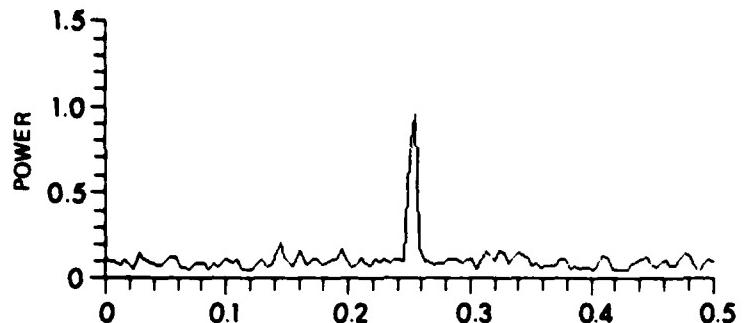
APPROXIMATION OF LR SPECTRUM WITH HSQ COEFFICIENT



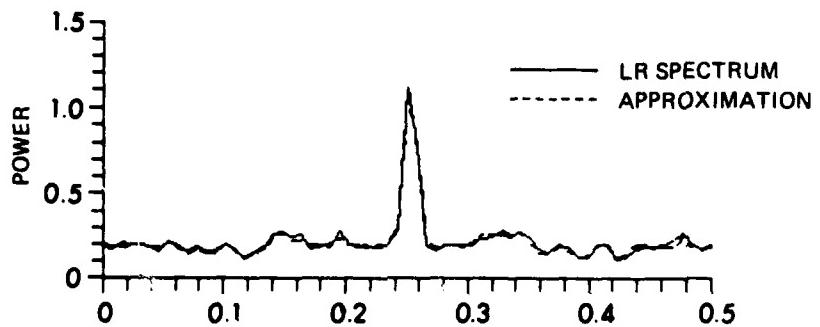
APPROXIMATION OF LR SPECTRUM WITH UNIFORM COEFFICIENT

FIGURE 10
COMPARISON OF POWER SPECTRA
2:1 REDUCTION, $L \times F = 32.200$

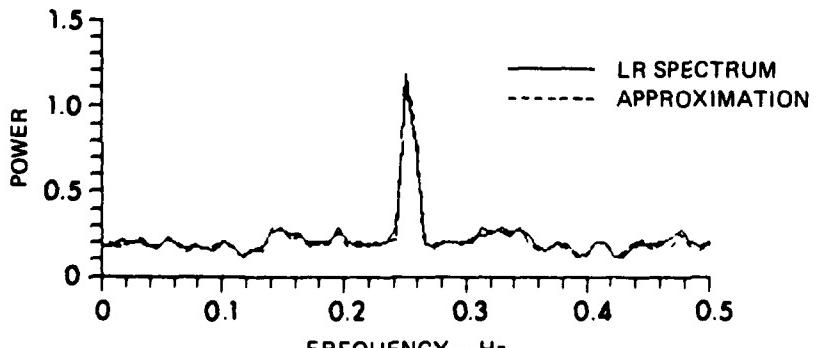
ARL:UT
AS-78-1496
CSP - GA
6-15-81



HIGH RESOLUTION SPECTRUM



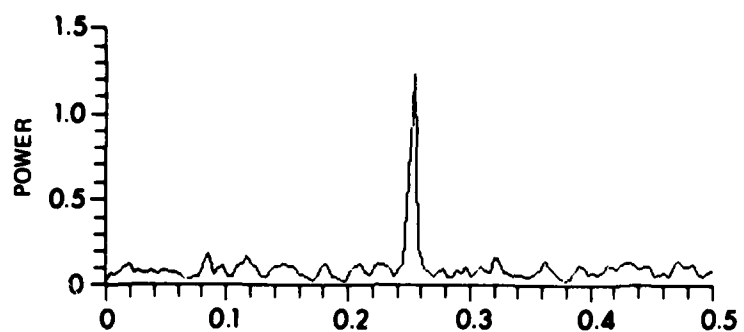
APPROXIMATION OF LR SPECTRUM WITH HSQ COEFFICIENT



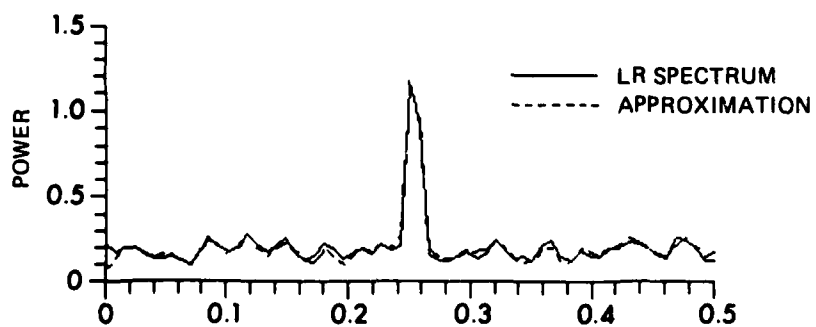
APPROXIMATION OF LR SPECTRUM WITH UNIFORM COEFFICIENT

FIGURE 11
COMPARISON OF POWER SPECTRA
2:1 REDUCTION, $L \times F = 32.300$

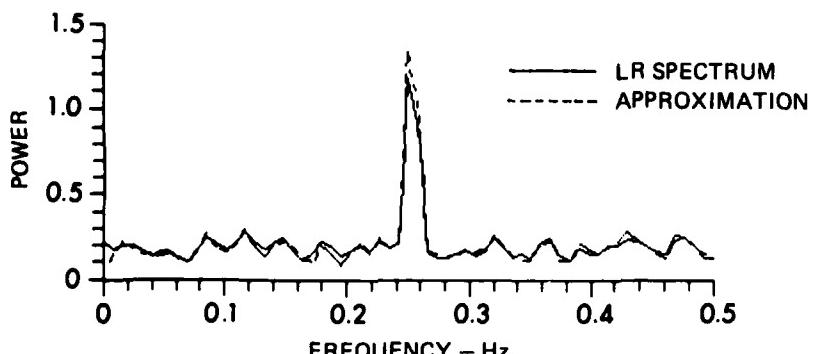
ARL:UT
AS-78-1497
CSP - GA
6-15-81



HIGH RESOLUTION SPECTRUM



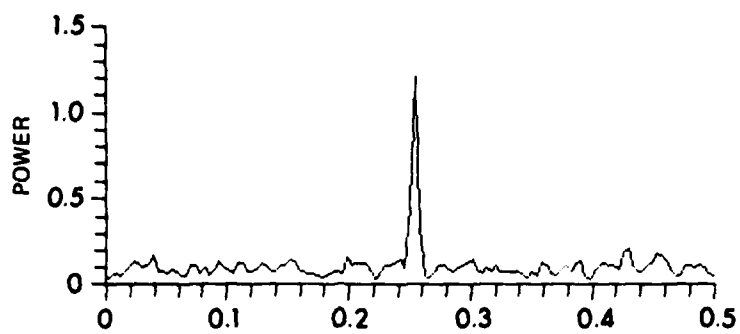
APPROXIMATION OF LR SPECTRUM WITH HSQ COEFFICIENT



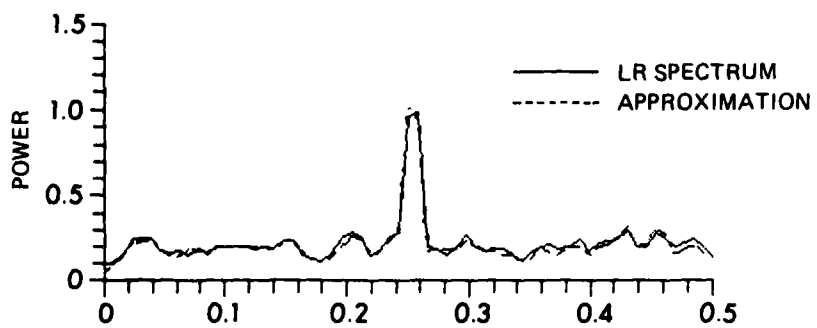
APPROXIMATION OF LR SPECTRUM WITH UNIFORM COEFFICIENT

FIGURE 12
COMPARISON OF POWER SPECTRA
2:1 REDUCTION, $L \times F = 32.400$

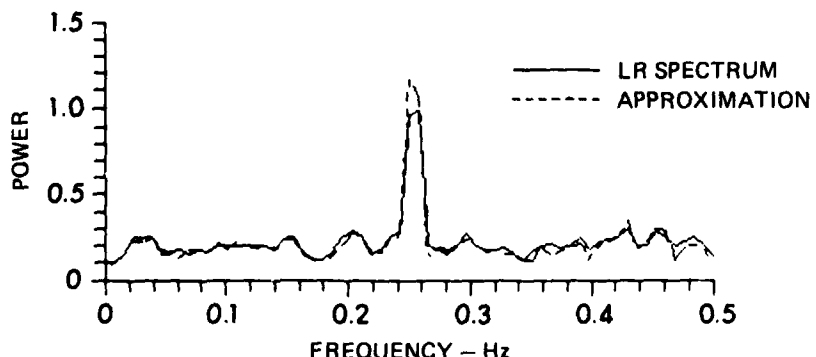
ARL:UT
AS-78-1498
CSP - GA
6-15-81



HIGH RESOLUTION SPECTRUM



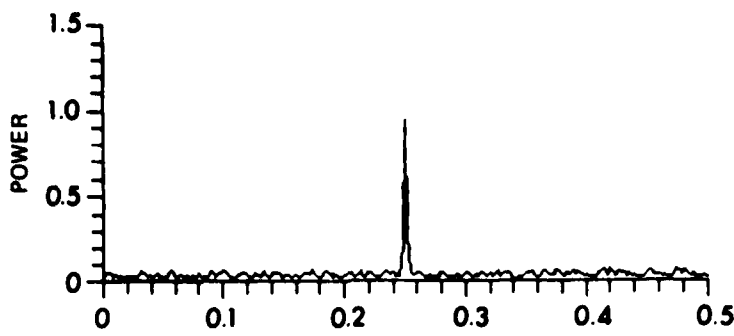
APPROXIMATION OF LR SPECTRUM WITH HSQ COEFFICIENT



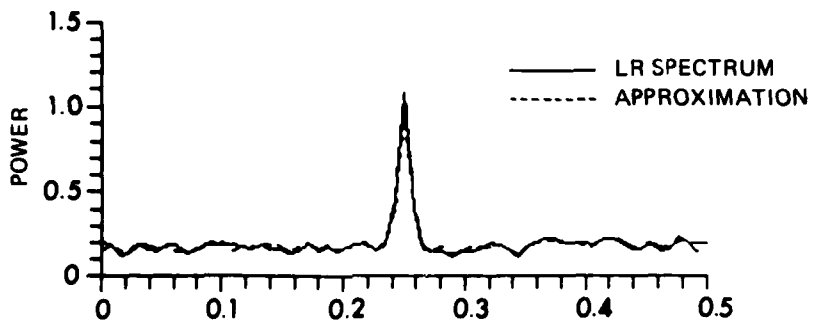
APPROXIMATION OF LR SPECTRUM WITH UNIFORM COEFFICIENT

FIGURE 13
COMPARISON OF POWER SPECTRA
2:1 REDUCTION, L x F = 32.500

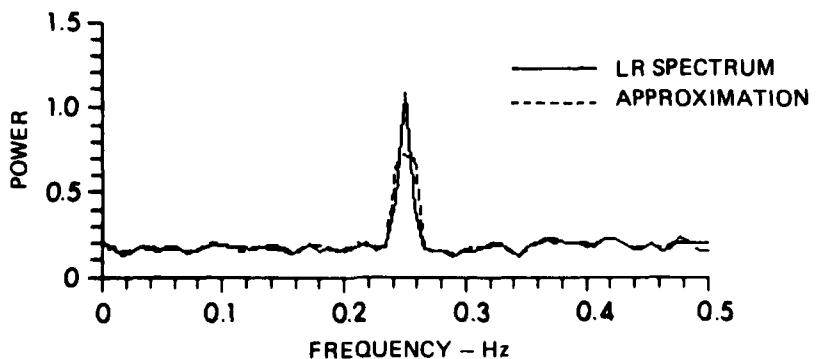
ARL:UT
AS-78-1499
CSP - GA
6-15-81



HIGH RESOLUTION SPECTRUM



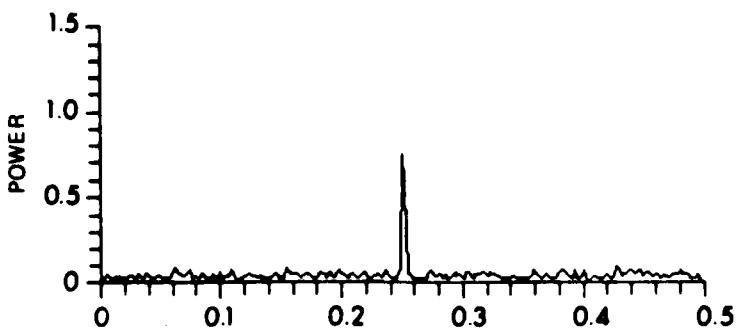
APPROXIMATION OF LR SPECTRUM WITH HSQ COEFFICIENT



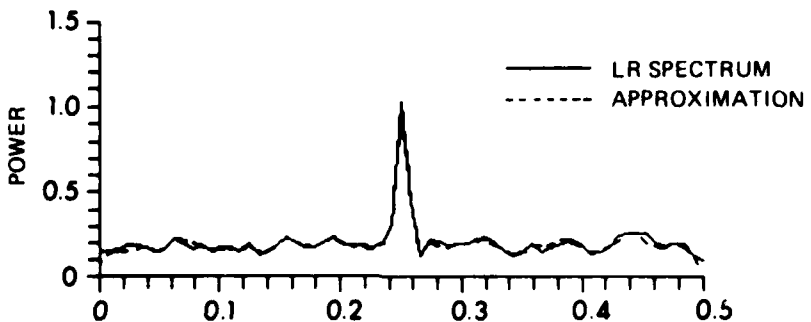
APPROXIMATION OF LR SPECTRUM WITH UNIFORM COEFFICIENT

FIGURE 14
COMPARISON OF POWER SPECTRA
4:1 REDUCTION, L x F = 32.000

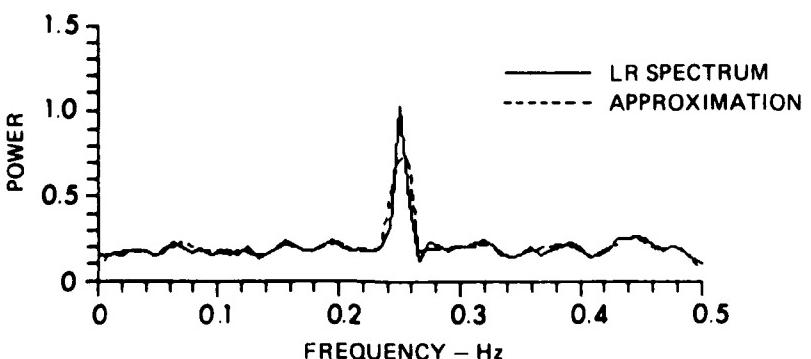
ARL:UT
AS-7B-1500
CSP - GA
6-15-81



HIGH RESOLUTION SPECTRUM



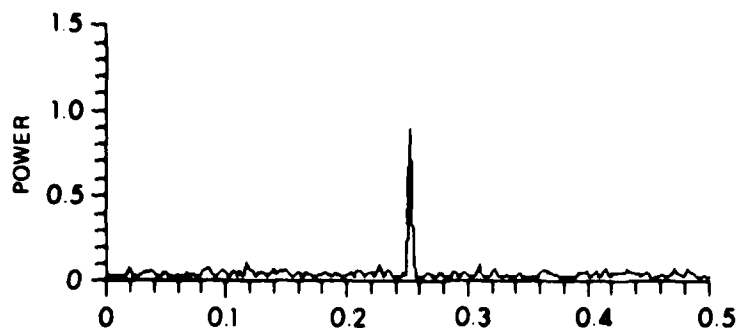
APPROXIMATION OF LR SPECTRUM WITH HSQ COEFFICIENT



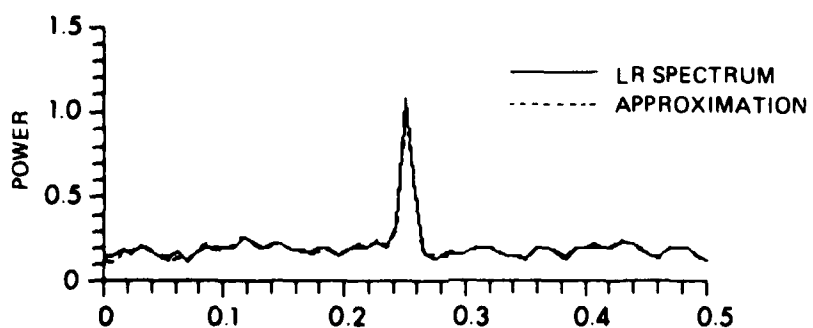
APPROXIMATION OF LR SPECTRUM WITH UNIFORM COEFFICIENT

FIGURE 15
COMPARISON OF POWER SPECTRA
4:1 REDUCTION, $L \times F = 32.100$

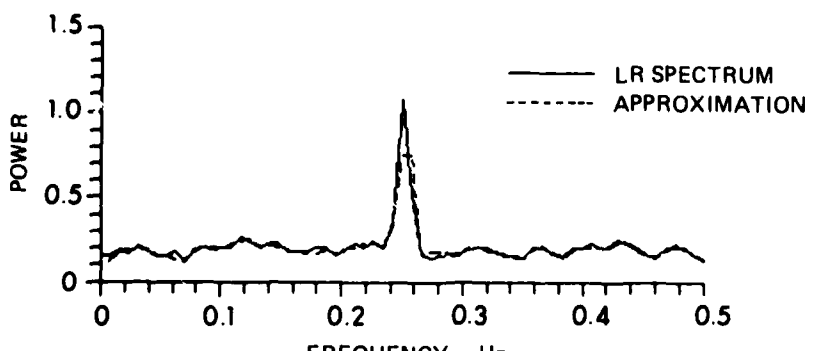
ARL:UT
AS-78-1501
CSP - GA
6-15-81



HIGH RESOLUTION SPECTRUM



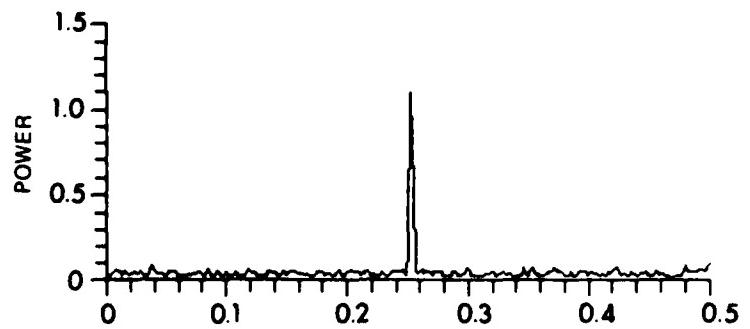
APPROXIMATION OF LR SPECTRUM WITH HSQ COEFFICIENT



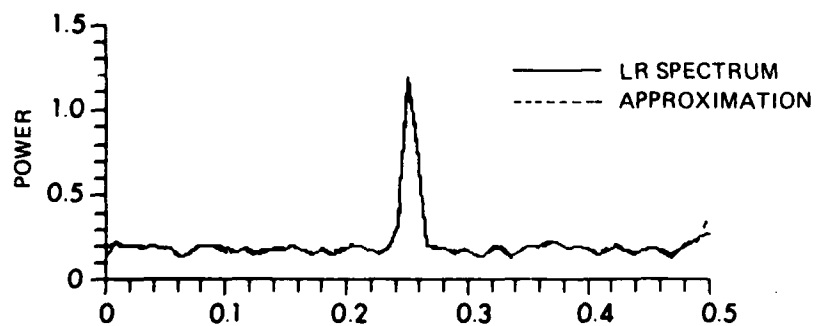
APPROXIMATION OF LR SPECTRUM WITH UNIFORM COEFFICIENT

FIGURE 16
COMPARISON OF POWER SPECTRA
4:1 REDUCTION, $L \times F = 32.200$

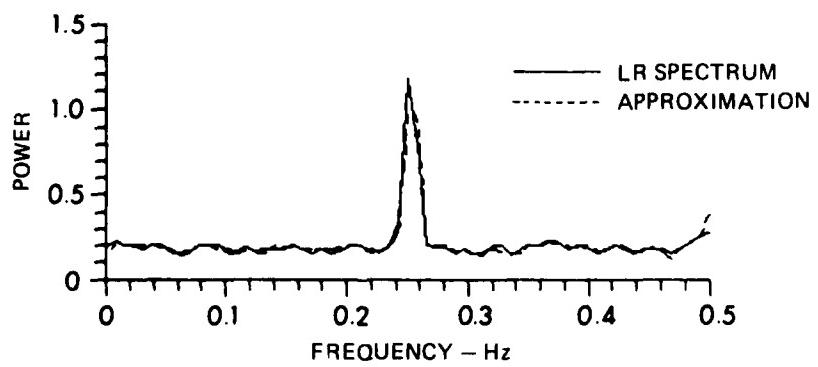
ARL:UT
AS-78-1502
CSP - GA
6-15-81



HIGH RESOLUTION SPECTRUM



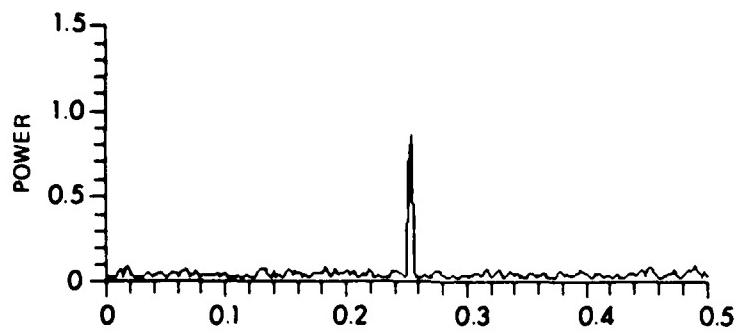
APPROXIMATION OF LR SPECTRUM WITH HSQ COEFFICIENT



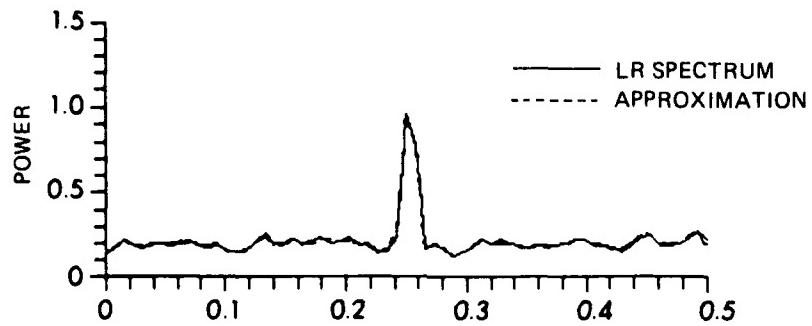
APPROXIMATION OF LR SPECTRUM WITH UNIFORM COEFFICIENT

FIGURE 17
COMPARISON OF POWER SPECTRA
4:1 REDUCTION, $L \times F = 32.300$

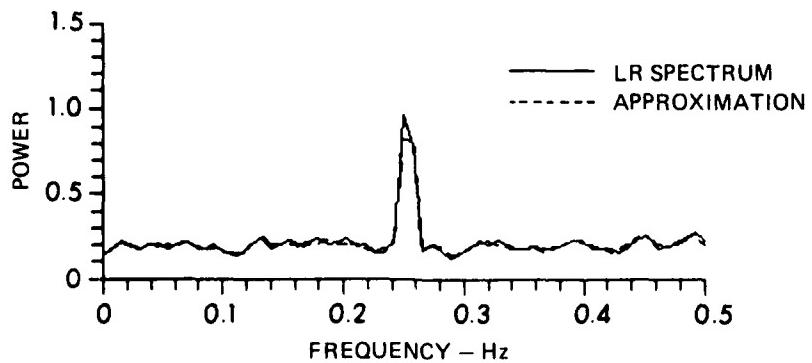
ARL:UT
AS-78-1503
CSP - GA
6-15-81



HIGH RESOLUTION SPECTRUM



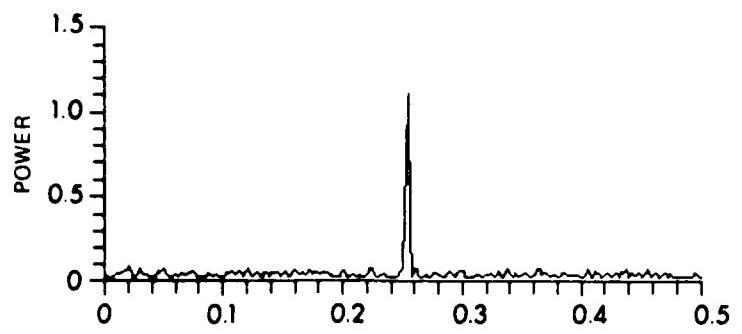
APPROXIMATION OF LR SPECTRUM WITH HSQ COEFFICIENT



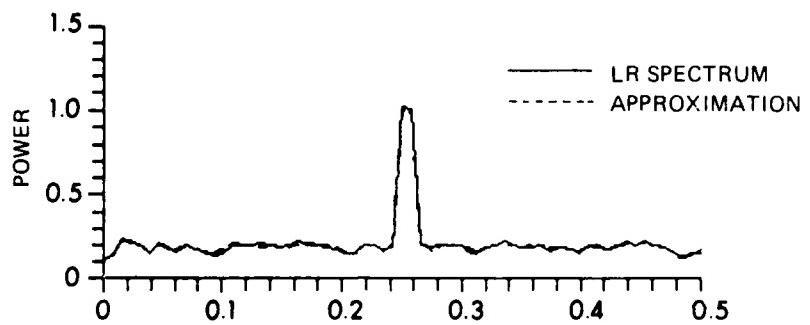
APPROXIMATION OF LR SPECTRUM WITH UNIFORM COEFFICIENT

FIGURE 18
COMPARISON OF POWER SPECTRA
4:1 REDUCTION, $L \times F = 32.400$

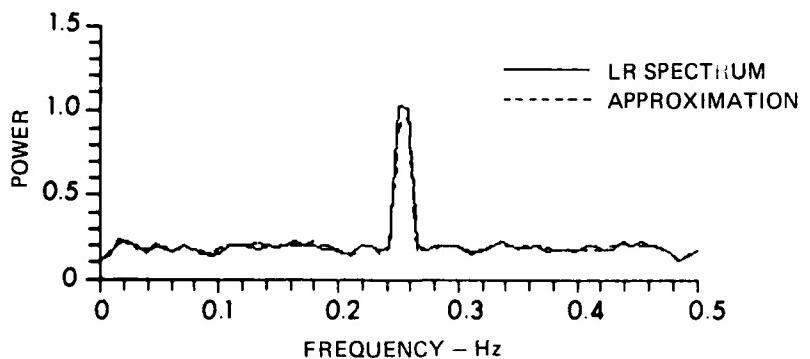
ARL:UT
AS-78-1504
CSP - GA
6-15-81



HIGH RESOLUTION SPECTRUM



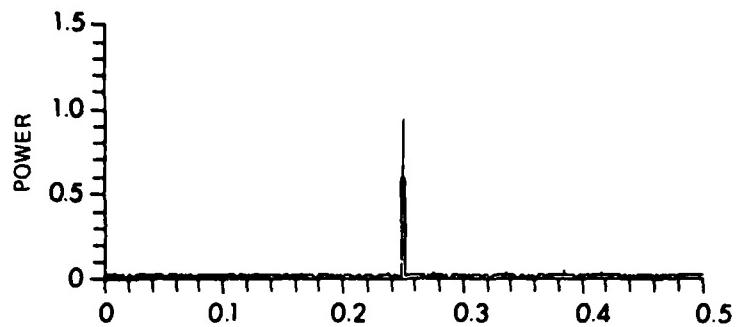
APPROXIMATION OF LR SPECTRUM WITH HSQ COEFFICIENT



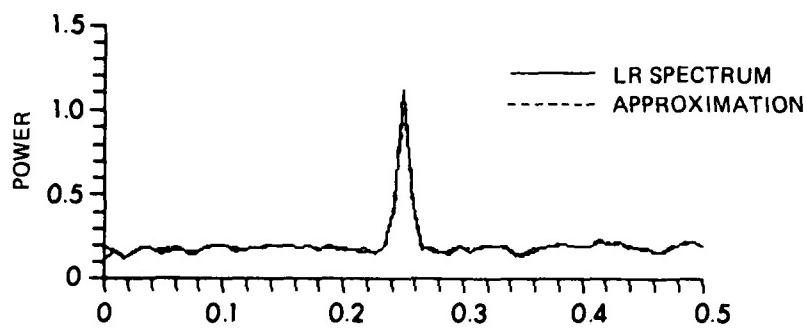
APPROXIMATION OF LR SPECTRUM WITH UNIFORM COEFFICIENT

FIGURE 19
COMPARISON OF POWER SPECTRA
4:1 REDUCTION, L x F = 32.500

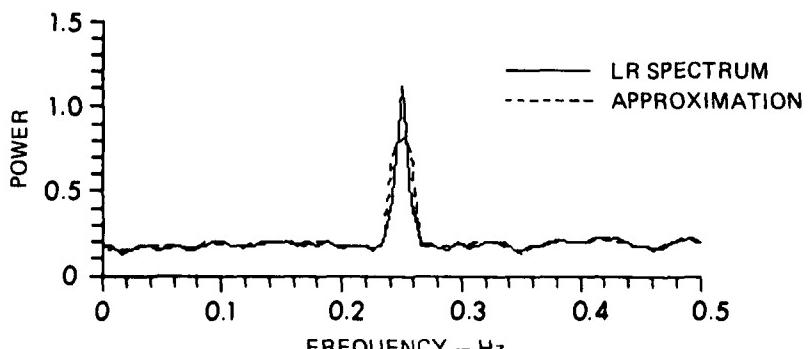
ARL:UT
AS-78-1505
CSP - GA
6-15-81



HIGH RESOLUTION SPECTRUM

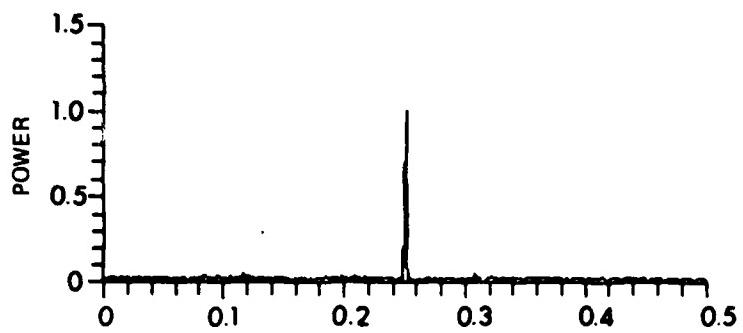


APPROXIMATION OF LR SPECTRUM WITH HSQ COEFFICIENT

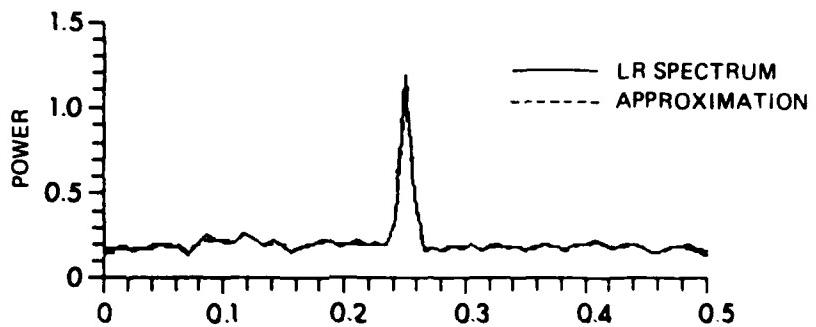


APPROXIMATION OF LR SPECTRUM WITH UNIFORM COEFFICIENT

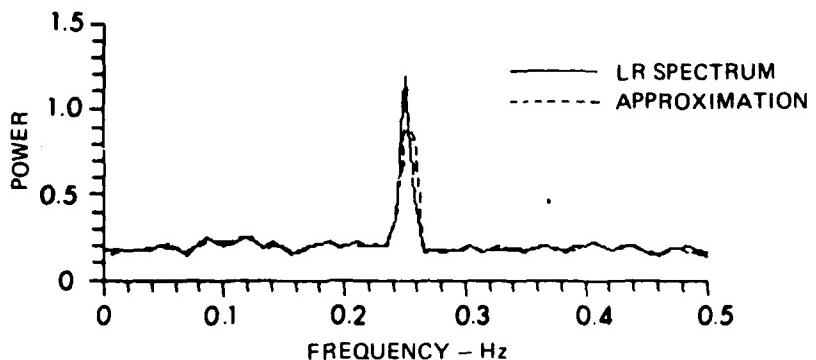
FIGURE 20
COMPARISON OF POWER SPECTRA
8:1 REDUCTION, $L \times F = 32.000$



HIGH RESOLUTION SPECTRUM



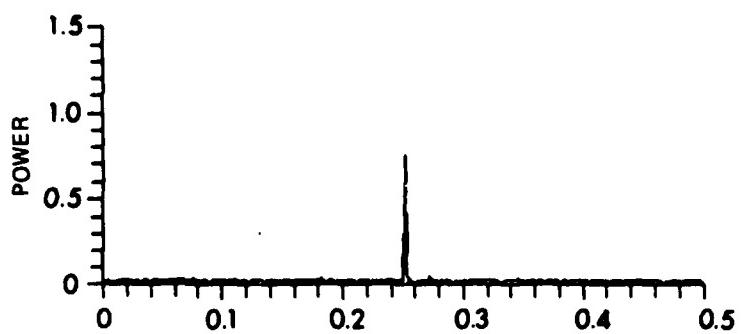
APPROXIMATION OF LR SPECTRUM WITH HSQ COEFFICIENT



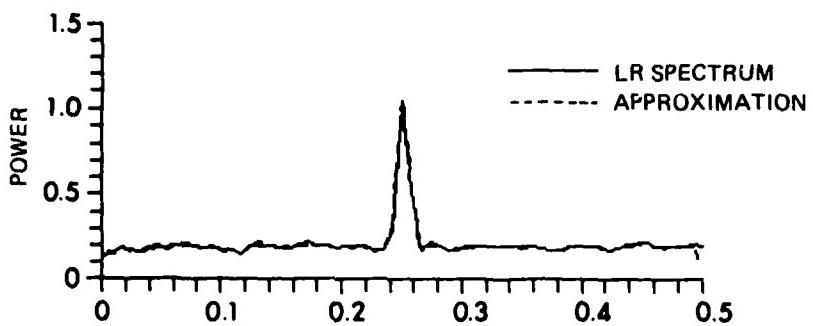
APPROXIMATION OF LR SPECTRUM WITH UNIFORM COEFFICIENT

FIGURE 21
COMPARISON OF POWER SPECTRA
8:1 REDUCTION, L x F = 32.100

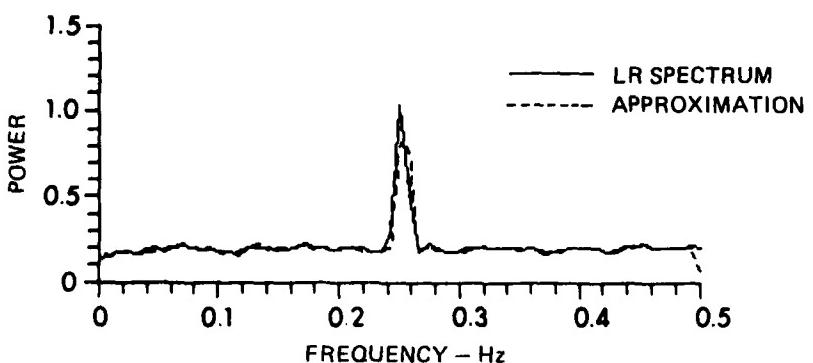
ARL:UT
AS-78-1507
CSP - GA
6-15-81



HIGH RESOLUTION SPECTRUM



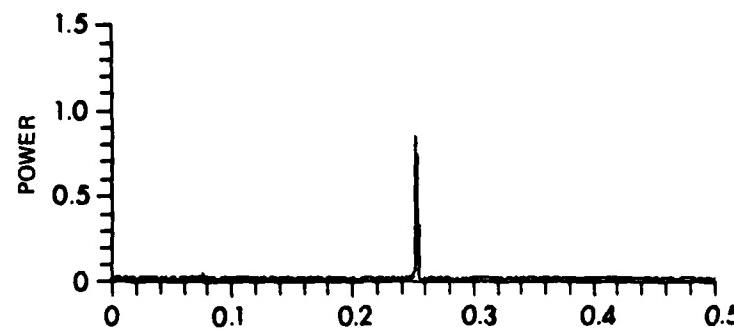
APPROXIMATION OF LR SPECTRUM WITH HSQ COEFFICIENT



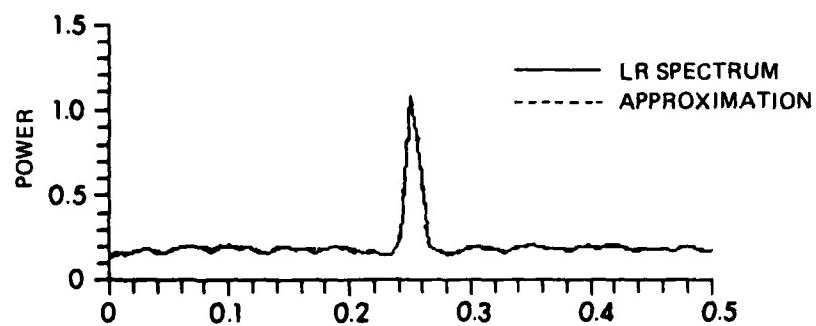
APPROXIMATION OF LR SPECTRUM WITH UNIFORM COEFFICIENT

FIGURE 22
COMPARISON OF POWER SPECTRA
8:1 REDUCTION, $L \times F = 32.200$

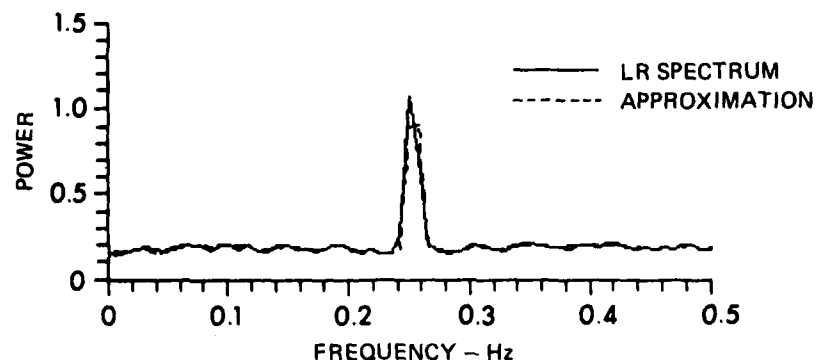
ARL:UT
AS-78-1508
CSP - GA
6-15-81



HIGH RESOLUTION SPECTRUM



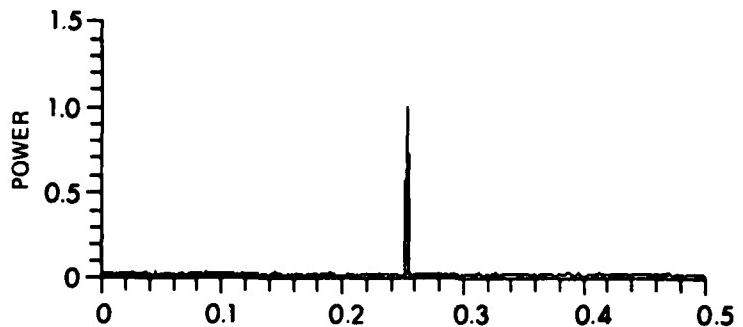
APPROXIMATION OF LR SPECTRUM WITH HSQ COEFFICIENT



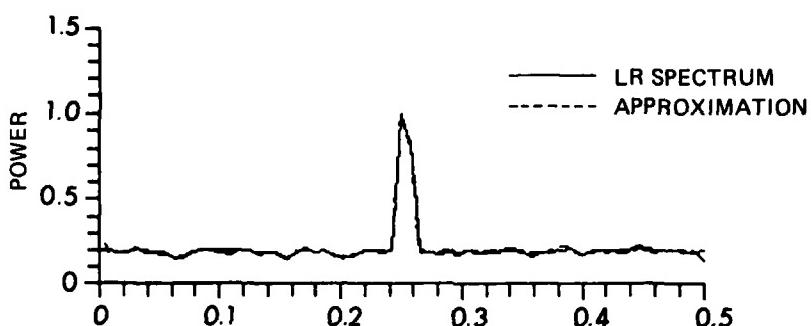
APPROXIMATION OF LR SPECTRUM WITH UNIFORM COEFFICIENT

FIGURE 23
COMPARISON OF POWER SPECTRA
8:1 REDUCTION, $L \times F = 32,300$

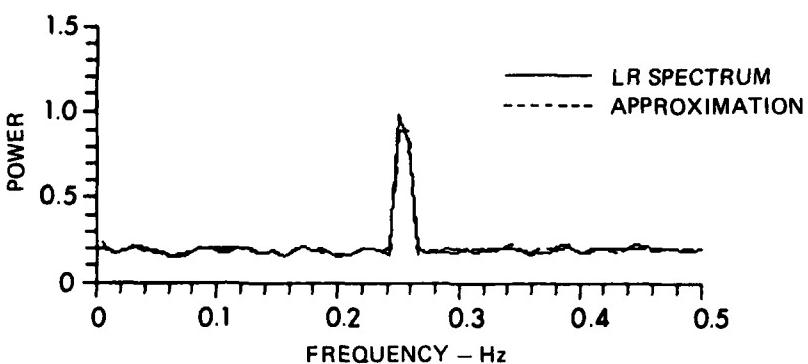
ARL:UT
AS-78-1509
CSP - GA
6-15-81



HIGH RESOLUTION SPECTRUM



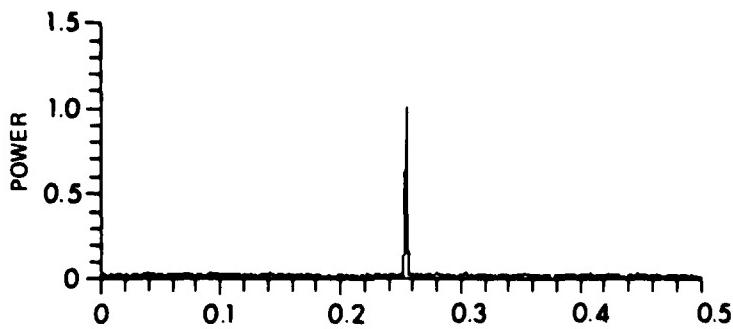
APPROXIMATION OF LR SPECTRUM WITH HSQ COEFFICIENT



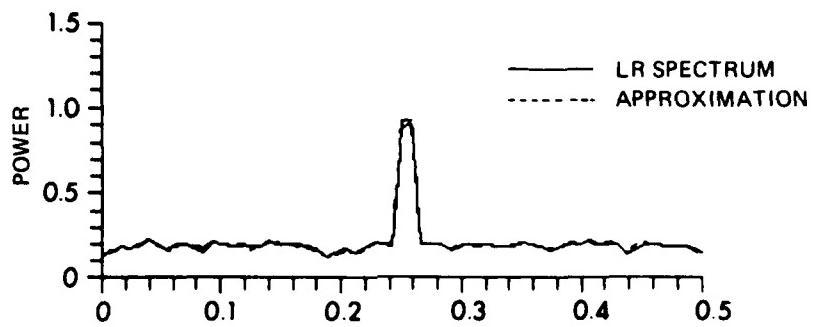
APPROXIMATION OF LR SPECTRUM WITH UNIFORM COEFFICIENT

FIGURE 24
COMPARISON OF POWER SPECTRA
8:1 REDUCTION, $L \times F = 32.400$

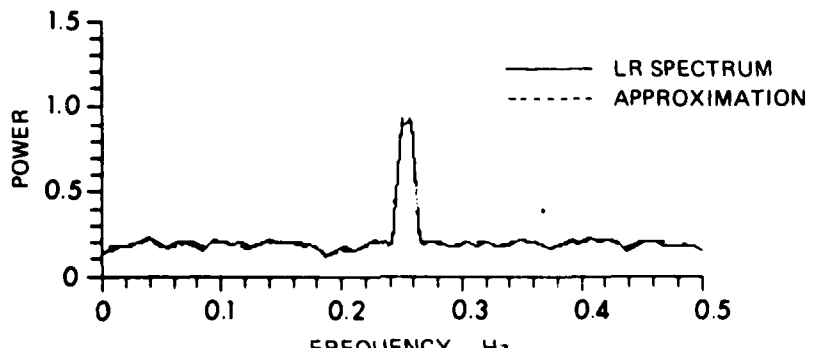
ARL:UT
AS-7B-1610
CSP - GA
6-15-81



HIGH RESOLUTION SPECTRUM



APPROXIMATION OF LR SPECTRUM WITH HSQ COEFFICIENT



APPROXIMATION OF LR SPECTRUM WITH UNIFORM COEFFICIENT

FIGURE 25
COMPARISON OF POWER SPECTRA
8:1 REDUCTION, $L \times F = 32.500$

ARL:UT
AS-78-1511
CSP - GA
6-15-81

will be symmetric in frequency around each FFT frequency, a representative idea of the effect of signal frequency on the behavior of the spectrum estimates can be had by varying normalized signal frequency between 32.0 and 32.5, for example. This was done in steps of 0.1 normalized frequency units for 2:1, 4:1, and 8:1 reduction ratios in the examples.

The amplitude normalization for the examples was chosen to preserve the amplitude of the signal for both the high and low resolution estimates. Since the noise power is uniformly distributed over frequency while the signal power is concentrated at a single frequency, increasing resolution spreads the noise power over a larger number of FFT frequencies. The signal, on the other hand, remains concentrated in a small number of FFT frequencies so the net result is a decrease in the amplitude of the mean noise level relative to the signal level. Since the spectra are normalized to preserve signal levels in the examples, the mean noise level in the low resolution estimates will be higher than in the high resolution estimates.

In each figure, the top plot is the high resolution spectrum from which the frequency averaged spectra are derived for both HSQ and uniform coefficients. In the middle plot are shown both the low resolution spectrum obtained by reprocessing the data with shorter transforms, and the frequency averaged spectrum obtained with HSQ coefficients. In the bottom plot, the same low resolution conventional spectrum is shown with the frequency averaged spectrum obtained using uniform coefficients. From the figures, it is quite clear that both sets of coefficients produce spectra which compare quite closely with the conventionally obtained spectrum.

IV.4 Signal Excess Comparison

To get a first order approximation of the gain or loss in ability to detect narrowband signals when frequency averaged spectra are used in place of conventionally obtained spectra, signal excess values were calculated for the examples. These values are presented in Figs. 26-28. They were obtained in the following manner. First, the high resolution spectrum, the low resolution spectrum, and both HSQ and uniform coefficient frequency averaged spectra were computed for a data sequence. Signal excess in dB was determined for all three of the low resolution spectra by referring the peak value of the spectrum to the known mean of the noise portion of the spectrum. This was repeated ten times on independent data sequences at each of 40 signal frequencies between FFT frequencies. The resulting average values of signal excess as a function of signal frequency are then shown in the top plots of Figs. 26-28 for 2:1, 4:1, and 8:1 resolution reduction ratios, respectively. In the bottom plots of these figures are shown the difference in signal excess between the conventional low resolution spectrum and the frequency averaged spectra.

The top plot in these figures shows the expected gradual decline in signal excess as the signal frequency approaches the midpoint between FFT frequencies. This is what is commonly referred to as the scalloping effect. In the bottom plot of Fig. 26 we see that the difference between the frequency averaged spectra and the conventional spectrum has the opposite shape, with a peak in the middle. This can be explained by examining the spectral windows in Fig. 5. Here it is seen that both of the frequency averaged spectral windows are somewhat

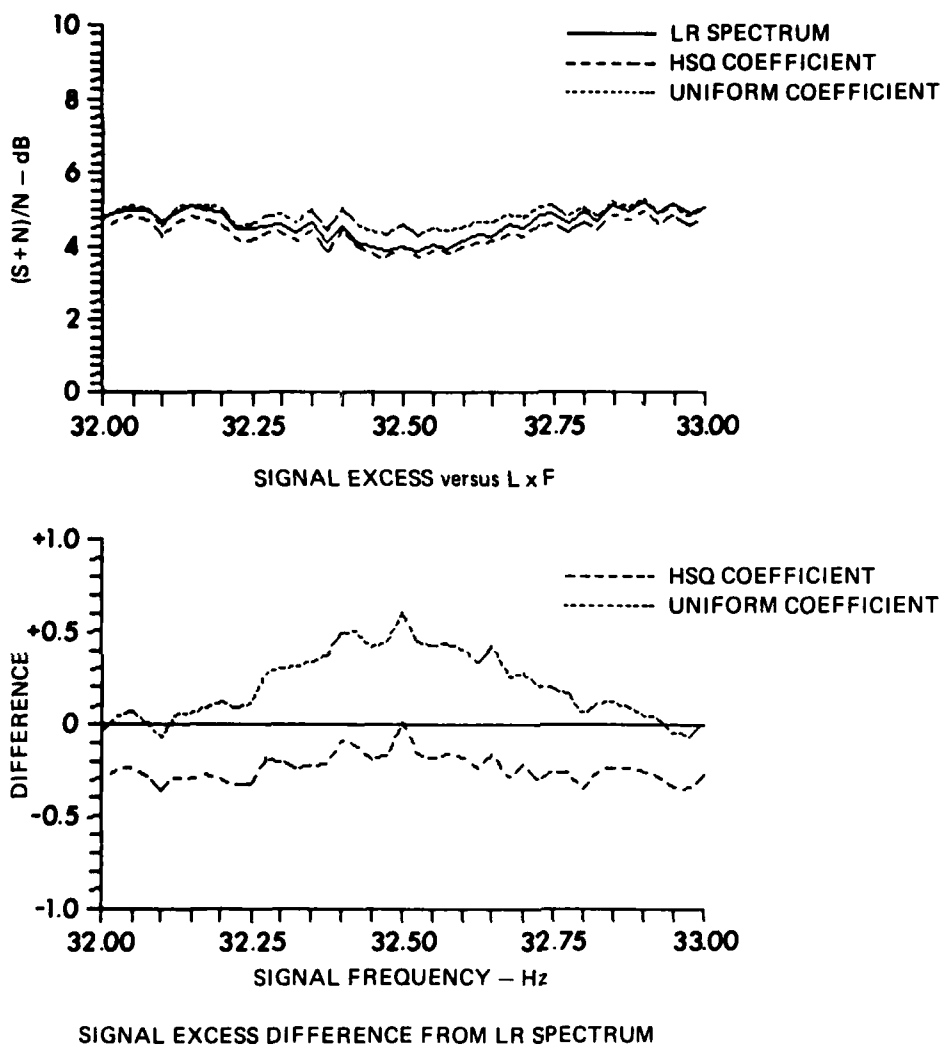


FIGURE 26
COMPARISON OF NORMALIZED SIGNAL EXCESS
2:1 REDUCTION

ARL:UT
AS-78-1512
CSP - GA
6-15-81

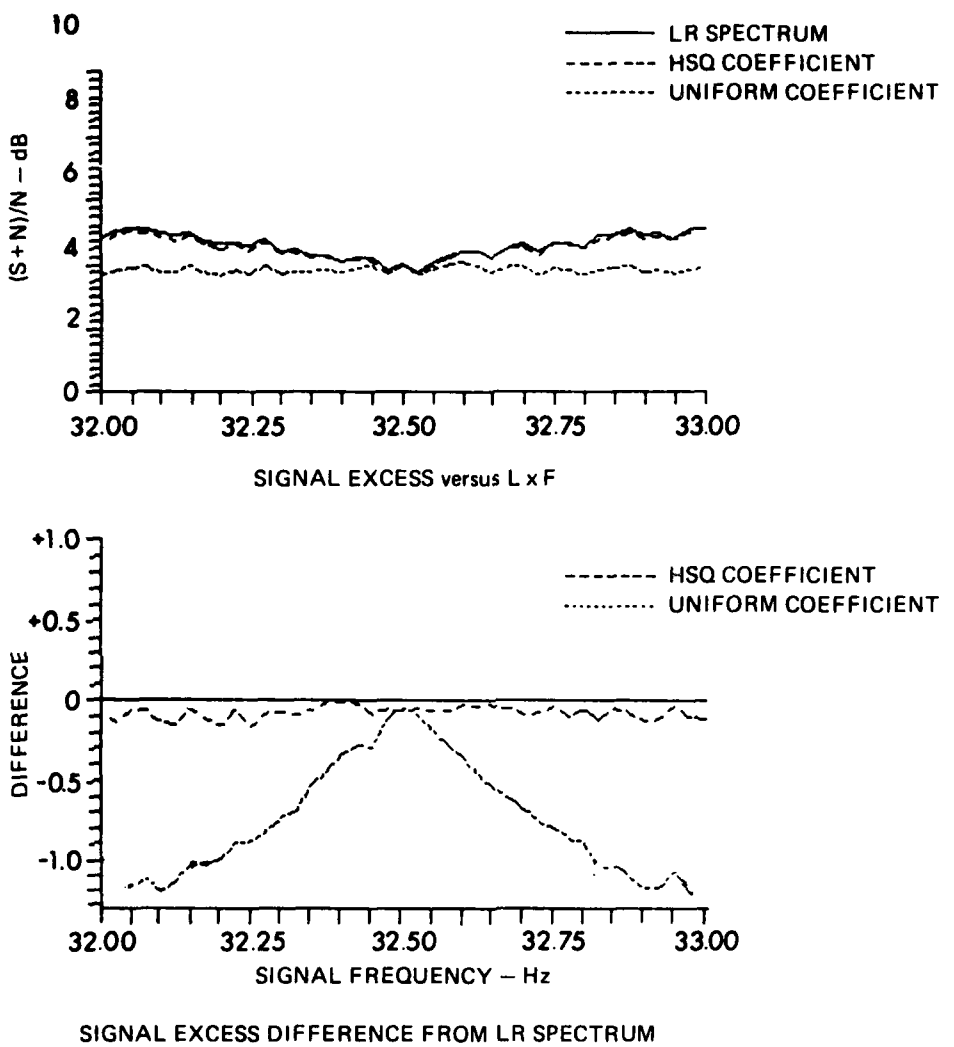


FIGURE 27
COMPARISON OF NORMALIZED SIGNAL EXCESS
4:1 REDUCTION

ARL:UT
 AS-78-1513
 CSP - GA
 6-15-81

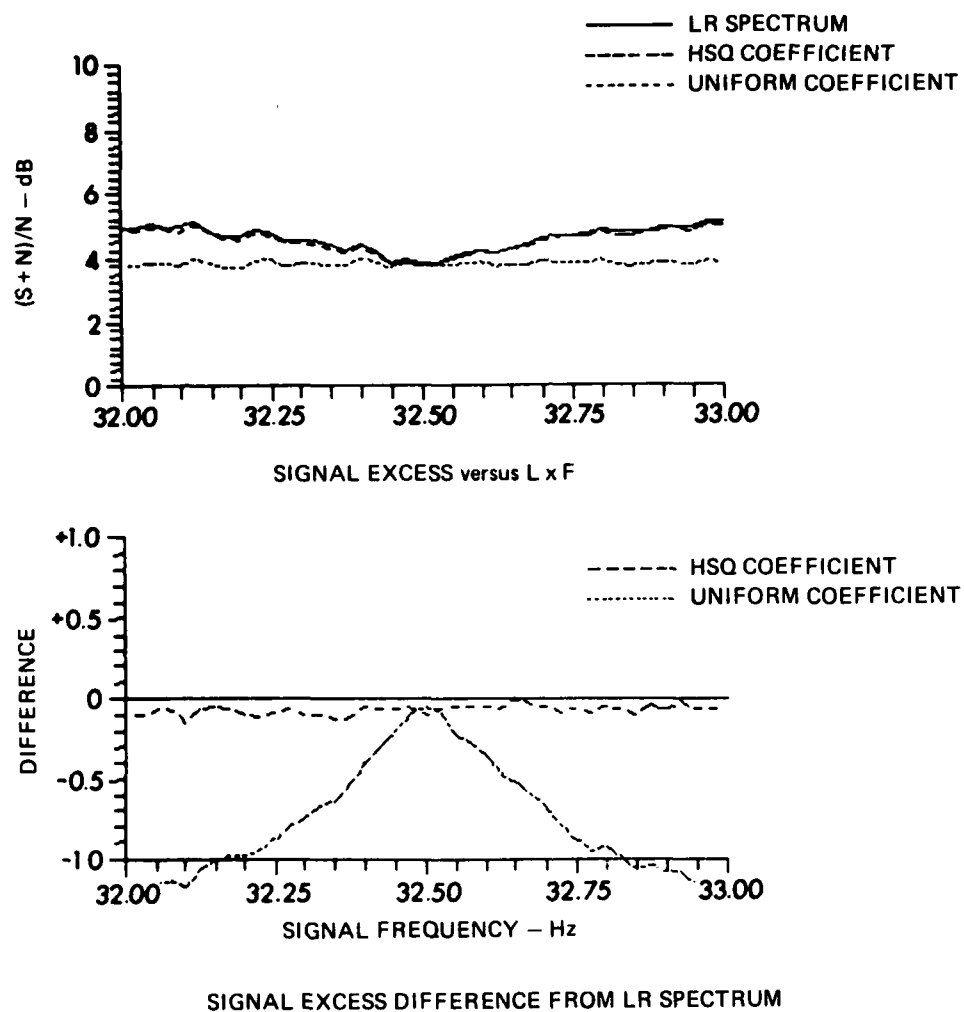


FIGURE 28
COMPARISON OF NORMALIZED SIGNAL EXCESS
8:1 REDUCTION

ARL:UT
AS-78-1514
CSP - GA
6-15-81

greater than the Hanning window at frequencies near the midpoint between FFT frequencies. We see that as the HSQ coefficient spectral window becomes a better approximation to the Hanning window at 4:1 and 8:1 reduction ratios, the signal excess difference in Figs. 27 and 28 becomes quite small. On the other hand, the differences between the Hanning window and the uniform coefficient window seen in Figs. 6 and 7 result in obvious signal excess differences. This suggests that the performance of a set of coefficients to be used in frequency averaging can be tested quickly by determining the associated spectral window and comparing it with the desired spectral window.

IV.5 Summary

In this chapter we have shown examples of frequency averaged spectra where our primary goal was to produce a lower resolution spectrum with characteristics as similar as possible to those of a low resolution spectrum obtained by reprocessing the original time series data. Both sets of coefficients yielded good results, with the HSQ coefficients holding a substantial advantage. In fact, the accuracy of the HSQ coefficient estimate can be improved still further by adjusting the value of α in Eq. (3.22).

We have pointed out the fact that the frequency averaging coefficients have a substantial impact on the effective spectral window of the frequency averaged spectrum. In Appendix 5 we show further examples where resolution reduction of 4:1 was done using four uniform coefficients. These examples, in which neither the number of equivalent degrees of freedom nor the effective spectral window match those of conventional processing, is included because it illustrates the most commonly employed technique. Some of the shortcomings of this technique are discussed in the appendix.

V. CONCLUSIONS

The results and examples presented here are by no means the last word on frequency averaging to achieve resolution reduction. However, they should form a sound basis of understanding for both current usage of frequency averaging techniques and for further development and exploration of these techniques.

As a basis for current usage, the report presents equations for calculating the number of equivalent degrees of freedom of frequency averaged spectra as a function of the coefficients used in the averaging process. Some guidance in the selection of coefficients is provided by the examples in Chapter IV and Appendix 5. Computer programs to numerically determine the spectral window associated with a set of coefficients can be easily written, enabling the use of the coefficients to tailor the window to suit particular needs. This capability for shaping the spectral window is itself a feature of the frequency averaging technique whose utility should be explored. Future work in this area should also examine the impact of signal bandwidth on these techniques.

APPENDIX 1

NOTES ON THE HANNING DATA WINDOW

Let $\text{rect}(x) = \begin{cases} 1 & , -\frac{1}{2} \leq x \leq \frac{1}{2} \\ 0 & , |x| > \frac{1}{2} \end{cases}$

Then the Hanning data window for a record of length L seconds extending from $t = -\frac{L}{2}$ to $t = \frac{L}{2}$ is defined as

$$w(t) = \frac{1}{2} \left\{ 1 + \cos \left(\frac{2\pi t}{L} \right) \right\} \text{rect}\left(\frac{t}{L}\right)$$

Let $W(f)$ be the Hanning spectral window defined by

$$W(f) = F\{w(t)\},$$

where F denotes the Fourier transform.

Then, using the asterisk to designate convolution,

$$\begin{aligned} W(f) &= \frac{1}{2} F\{1 + \cos(2\pi t/L)\} * F\{\text{rect}(t/L)\} \\ &= \frac{1}{2} \left[\delta(f) + \frac{1}{2} \delta(f - \frac{1}{L}) + \frac{1}{2} \delta(f + \frac{1}{L}) \right] * \left[L \frac{\sin(\pi Lf)}{\pi Lf} \right] \\ &= \frac{1}{2} \left[\frac{L \sin(\pi Lf)}{\pi Lf} + \frac{L \sin[\pi L(f - \frac{1}{L})]}{2\pi L(f - \frac{1}{L})} + \frac{L \sin[\pi L(f + \frac{1}{L})]}{2\pi L(f + \frac{1}{L})} \right] \\ &= \frac{\sin(\pi Lf)}{2\pi} \left[\frac{1}{f} - \frac{1}{2} \left(\frac{L}{Lf-1} + \frac{L}{Lf+1} \right) \right] \\ &= \frac{L \text{sinc}(Lf)}{2[1-(Lf)^2]} \end{aligned}$$

where $\text{sinc}(x) = \sin(\pi x)/\pi x$. The usual procedure is to normalize the data window so that

$$W(f) = \frac{\text{sinc}(Lf)}{1 - (Lf)^2} .$$

In many cases of practical interest, the data window extends from $t=0$ to $t=L$:

$$w'(t) = w(t - \frac{L}{2}) .$$

Then

$$W'(f) = F\{w'(t)\}$$

$$= e^{-i\pi L f} W(f) .$$

Since discrete transforms are generally used to process data, we will be interested in $W'(f)$ evaluated at $f_k = k/L$ for integer values of k :

$$W'(f_k) = \begin{cases} \frac{L}{2} , & k=0 \\ -\frac{L}{4} , & k = \pm 1 \\ 0 , & |k| > 1 \end{cases} .$$

The convenient discrete form of $W'(f_k)$ allows us to implement the data window by convolving the rectangular windowed data with the sequence $(-\frac{L}{4}, \frac{L}{2}, -\frac{L}{4})$, or, where normalization is used, with $(-\frac{1}{4}, \frac{1}{2}, -\frac{1}{4})$. For example, if $i = \sqrt{-1}$ and

$$X_j = A_j + iB_j$$

is the complex discrete transform of the sequence x_k , where the rectangular data window has been used, we can form the complex Hanned transform X_j^k , by

$$x_j^k = -\frac{1}{4} x_{j-1} + \frac{1}{2} x_j - \frac{1}{4} x_{j+1} \quad .$$

This is frequently more convenient than multiplying the data sequence by the discrete version of $w(t)$ before transforming.

APPENDIX 2

STATISTICAL STABILITY OF LOW RESOLUTION SPECTRA DERIVED FROM
NON-OVERLAPPED HIGHER RESOLUTION FFTs

In this appendix we will assume that we have data which consists of a sample function from a discrete stationary zero mean white Gaussian noise process. From this data we will extract a number P of non-overlapping segments, each of which will be discrete transformed with the Hanning window applied. An estimate of the power spectrum of the process will be obtained from each discrete transform and the resulting P spectrum estimates will be averaged to form what will be referred to as the high resolution spectrum estimate. From this estimate, a lower resolution estimate will be obtained by means of the frequency averaging techniques. Our objective here is to obtain an expression for the number of equivalent degrees of freedom of the lower resolution estimate.

Let $C_p(f_j)$ be the high resolution estimate obtained from the p^{th} segment of data, where $f_j = (j-1)/L\Delta$, L being the length of the discrete transform and Δ being the sampling interval of the process. Then, the lower resolution estimate obtained by frequency averaging is

$$\hat{C}(f_j) = \sum_{k=-K}^{K} a_k \left\{ \frac{1}{P} \sum_{p=1}^P C_p(f_{j-k}) \right\} \quad (\text{A-2.1})$$

$$= \frac{1}{P} \sum_{p=1}^P \left\{ \sum_{k=-K}^{K} a_L C_p(f_{j-k}) \right\} \quad (\text{A-2.2})$$

Since the random variables $C_p(f_i)$ are independent and identically distributed over $1 \leq p \leq P$, the following lemma will prove useful.

Lemma. Let Z_1, \dots, Z_p be independent identically distributed random variables, not necessarily Chi-square. Let

$$v = \frac{2E^2 Z_1}{\text{Var } Z_1}$$

be the number of equivalent degrees of freedom of each Z_i . Further, let

$$Z = \frac{1}{P} \sum_{i=1}^P Z_i .$$

Then the number of equivalent degrees of freedom of Z is Pv .

Proof. The number of equivalent degrees of freedom of Z is

$$\frac{2E^2 Z}{\text{Var } Z} = \frac{2E^2 \left\{ \frac{1}{P} \sum_{i=1}^P Z_i \right\}}{\text{Var} \left\{ \frac{1}{P} \sum_{i=1}^P Z_i \right\}}$$

$$= \frac{2E^2 Z_1}{\frac{1}{P} \text{Var } Z_1}$$

$$= Pv ,$$

which completes the proof.

We can now compute the number of equivalent degrees of freedom of $\hat{C}(f_j)$ by computing the number of equivalent degrees of freedom for the bracketed term in Eq. (A-2.2) for $p=1$, and invoking the lemma. For simplicity, let

$$C(f_j) = C_1(f_j) \quad (A-2.3)$$

be the spectrum estimate based on the first segment of the data, or x_1, \dots, x_L . Let X_j , $1 \leq j \leq L$, be the discrete transform of the data, and let

$$X_j = A_j + iB_j , \quad (A-2.4)$$

where $i = \sqrt{-1}$. As pointed out in Chapter 2, the A_j and B_j , $1 \leq j \leq L$, are independent zero mean Gaussian with a variance which we will denote σ^2 . Applying the Hanning window via a convolution in the frequency domain, we have

$$A_j = -0.25 A_{j-1} + 0.5 A_j - 0.25 A_{j+1} \quad (A-2.5a)$$

$$B_j = -0.25 B_{j-1} + 0.5 B_j - 0.25 B_{j+1} \quad (A-2.5b)$$

$$X_j = A_j + iB_j . \quad (A-2.5c)$$

Then the estimate $C(f_j)$ is given by

$$\begin{aligned} C(f_j) &= L\Delta |X_j|^2 \\ &= L\Delta (A_j^2 + B_j^2) . \end{aligned} \quad (A-2.6)$$

Without loss of generality, we can assume $L\Delta=1$, since multiplication of a random variable by a constant does not alter its number of equivalent degrees of freedom. Also, by assuming that A_0, \dots, A_{N+1} and B_0, \dots, B_{N+1} are independent zero mean Gaussian with variance σ^2 , we can restate our objective as the calculation of the equivalent degrees of freedom of

$$Q = \sum_{k=1}^N a_k (A_k^2 + B_k^2) \quad (A-2.7)$$

where A_k and B_k are defined in Eq. (A-2.5). Applying Eq. (2.26) and the lemma we have for the number of equivalent degrees of freedom of $\hat{C}(f_j)$,

$$v = \frac{2PE^2 Q}{\text{Var } Q} \quad (A-2.8)$$

$$= \frac{2PE^2 \left\{ \sum_{k=1}^N a_k A_k^2 + \sum_{k=1}^N a_k B_k^2 \right\}}{\text{Var} \left\{ \sum_{k=1}^N a_k A_k^2 + \sum_{k=1}^N a_k B_k^2 \right\}} \quad (A-2.9)$$

$$= \frac{4PE^2 \left\{ \sum_{k=1}^N a_k A_k^2 \right\}}{\text{Var} \left\{ \sum_{k=1}^N a_k A_k^2 \right\}} . \quad (A-2.10)$$

Since $\sum a_k A_k^2$ and $\sum a_k B_k^2$ are independent and identically distributed.

Expanding Eq. (A-2.10) yields

$$v = \frac{4PE^2 A_1^2 \left[\sum_{k=1}^N a_k \right]^2}{\sum_{k=1}^N \sum_{j=1}^N a_k a_j E \left\{ A_k^2 A_j^2 \right\} - E^2 A_1^2 \left[\sum_{k=1}^N a_k \right]^2}, \quad (A-2.11)$$

since the A_k are identically distributed. Some fairly tedious computation can be employed to show that

$$EA_k^2 = 3.750 \times 10^{-1} \sigma^2, \quad 1 \leq k \leq N, \quad (A-2.12)$$

and

$$EA_k^2 A_j^2 = \begin{cases} 4.219 \times 10^{-1} \sigma^4, & k=j \\ 2.656 \times 10^{-1} \sigma^4, & |k-j| = 1 \\ 1.484 \times 10^{-1} \sigma^4, & |k-j| = 2 \\ 1.406 \times 10^{-1} \sigma^4, & |k-j| \geq 3 \end{cases}. \quad (A-2.13)$$

As an example, when uniform weighting coefficients c_i are used,

$$v = \begin{cases} 2, & N = 1 \\ 2.77, & N = 2 \\ 3.72, & N = 3 \end{cases}, \quad (A-2.14)$$

and, for $N \geq 4$ in this case, Eq. (A-2.11) reduces to

$$v = \frac{5.625 \times 10^{-1} N^2}{5.469 \times 10^{-1} N - 2.813 \times 10^{-1}} . \quad (A-2.15)$$

APPENDIX 3

THE EFFECTS OF THE HANNING WINDOW ON FREQUENCY AUTOCOVARIANCE

Let x_1, \dots, x_L be independent zero mean Gaussian random variables with variance σ^2 , and let X_1, \dots, X_L be their discrete Fourier transform where

$$X_j = A_j + iB_j . \quad (A-3.1)$$

As pointed out in Chapter 2, the random variables A_j and B_j are independent zero mean Gaussian with variance $\frac{\sigma^2}{2L}$ for $1 \leq j \leq \frac{L}{2}$. The corresponding spectrum estimate is

$$\begin{aligned} C(f_j) &= L\Delta |X_j|^2 \\ &= L\Delta (A_j^2 + B_j^2) . \end{aligned} \quad (A-3.2)$$

The frequency autocovariance is then

$$\begin{aligned} \text{Cov}\{C(f_j), C(f_i)\} &= E\left\{[C(f_j) - E\{C(f_j)\}][C(f_i) - E\{C(f_i)\}]\right\} \\ &= E\{C(f_j) C(f_i)\} - E\{C(f_j)\} E\{C(f_i)\} . \end{aligned} \quad (A-3.3)$$

Note that for $i \neq j$, $C(f_i)$ and $C(f_j)$ are independent, hence their covariance is zero. If $i=j$,

$$\text{Cov}\{C(f_j), C(f_i)\} = \text{Var}\{C(f_j)\}$$

$$= \sigma^4 \Delta^2 ,$$

from Eq. (2.13). Hence, for a single transform estimate of the spectrum,

$$\text{Cov}\{C(f_j), C(f_i)\} = \begin{cases} \sigma^4 \Delta^2 & , i = j \\ 0 & , i \neq j \end{cases} . \quad (\text{A-3.4})$$

In similar fashion, if $\bar{C}(f_j)$ is the estimate which results from averaging P non-overlapped transforms, we can show

$$\text{Cov}\{\bar{C}(f_j), \bar{C}(f_i)\} = \begin{cases} \frac{\sigma^4 \Delta^2}{P} & , i = j \\ 0 & , i \neq j \end{cases} . \quad (\text{A-3.5})$$

Suppose now that we apply the Hanning data window via convolution (see Appendix 1). Then the complex Hanned transform is

$$X_j = A_j + iB_j , \quad (\text{A-3.6})$$

where

$$A_j = -0.25A_{j-1} + 0.5A_j - 0.25A_{j+1} , \quad (\text{A-3.7a})$$

$$B_j = -0.25B_{j-1} + 0.5B_j - 0.25B_{j+1} . \quad (\text{A-3.7b})$$

The Hanned spectrum estimate is

$$\begin{aligned} C(f_j) &= L\Delta |X_j|^2 \\ &= L\Delta (A_j^2 + B_j^2) . \end{aligned} \quad (\text{A-3.8})$$

As before, the frequency autocovariance is

$$\begin{aligned}\text{Cov}\{\mathcal{C}(f_j), \mathcal{C}(f_i)\} &= E\{\mathcal{C}(f_j) \mathcal{C}(f_i)\} - E\{\mathcal{C}(f_j)\} E\{\mathcal{C}(f_i)\} \\ &= 2L^2 \Delta^2 \left[E\left\{A_j^2 A_i^2\right\} - E\left\{A_j^2\right\} E\left\{A_i^2\right\} \right] .\end{aligned}\quad (\text{A-3.9})$$

This equation can be evaluated with the help of Appendix 2, bearing in mind that in this appendix the variance of A_i and B_i is $\frac{\sigma^2}{2L}$ instead of σ^2 .

$$\text{Cov}\{\mathcal{C}(f_j), \mathcal{C}(f_i)\} = \begin{cases} 1.406 \times 10^{-1} \sigma^4 \Delta^2 , & i=j \\ 6.250 \times 10^{-2} \sigma^4 \Delta^2 , & |i-j| = 1 \\ 3.907 \times 10^{-3} \sigma^4 \Delta^2 , & |i-j| = 2 \\ 0 , & |i-j| \geq 3 \end{cases} . \quad (\text{A-3.10})$$

As before, since non-overlapped data segments are independent, when P non-overlapped Hanned spectrum estimates are averaged,

$$\text{Cov}\{\bar{\mathcal{C}}(f_j), \bar{\mathcal{C}}(f_i)\} = \begin{cases} 1.406 \times 10^{-1} \frac{\sigma^4 \Delta^2}{P} , & i=j \\ 6.250 \times 10^{-2} \frac{\sigma^4 \Delta^2}{P} , & |i-j| = 1 \\ 3.907 \times 10^{-3} \frac{\sigma^4 \Delta^2}{P} , & |i-j| = 2 \\ 0 , & |i-j| \geq 3 \end{cases} . \quad (\text{A-3.11})$$

APPENDIX 4

STABILITY OF ESTIMATED LOW RESOLUTION SPECTRA DERIVED FROM
FIFTY PERCENT OVERLAPPED HIGHER RESOLUTION FFTs

In this appendix we will generalize the results from Appendix 2 to the case where the high resolution spectrum estimate is derived from overlapped transforms. In particular, we will assume that the data has been divided into P segments where the last half of each segment overlaps the first half of the succeeding one. These segments are then windowed and transformed, and the resulting P spectra are averaged to form the high resolution spectrum estimate. The low resolution estimate is then derived from the high resolution estimate by means of the frequency averaging techniques.

The following notation will be used in this appendix. Let $x(t)$ be a realization of a stationary random process with power spectral density $S(f)$. Let $C_p(f_j)$ be the discrete spectrum estimate based on the p^{th} segment of data. ($C_p(f_j)$ is formed as described in Chapter II by sampling the windowed data segment and doing a discrete transform with an FFT algorithm.) Then the high resolution estimate of $S(f_j)$ is

$$C(f_j) = \frac{1}{P} \sum_{p=1}^P C_p(f_j) . \quad (\text{A-4.1})$$

The frequency averaging techniques are employed to produce a low resolution estimate of $S(f_k)$ defined by

$$\hat{C}(f_k) = \sum_{j=-K}^K a_j C(f_{k-j}) , \quad (A-4.2)$$

where the a_j are called the window coefficients for the frequency averaging on the high resolution spectrum. In order to compute the number of equivalent degrees of freedom v of $\hat{C}(f_k)$, we will compute its mean and variance and make use of Eq. (2.26):

$$v = \frac{2E\{\hat{C}(f_k)\}}{\text{Var}\{\hat{C}(f_k)\}} . \quad (A-4.3)$$

We first compute the mean:

$$\begin{aligned} E\{\hat{C}(f_k)\} &= E\left\{\sum_{j=-K}^K a_j C(f_{k-j})\right\} \\ &= \frac{1}{P} \sum_{p=1}^P \sum_{j=-K}^K a_j E\{C_p(f_{k-j})\} . \end{aligned} \quad (A-4.4)$$

To compute $E[C_p(f_{k-j})]$ we must introduce further notation. Let $w(t)$ be the data window, centered about the origin, and let L denote the length of each FFT in seconds. Then $C_p(f_{k-j})$ is the result of transforming the function $x(t)w(t-\frac{L}{2}p)$. To simplify matters, we will use continuous transform notation, the underlying assumption being that the results will not differ significantly if the sampling frequency is high enough to prevent corruption of the discrete transforms by aliasing. Then, from the autocorrelation theorem we have

$$E\{C_p(f_{k-j})\} = \iint E\{x(u)x^*(v)\} w(u - \frac{L_p}{2}) w^*(v - \frac{L_p}{2}) e^{-i2\pi(u-v)f_{k-j}} du dv, \quad (A-4.5)$$

where all integrals, unless otherwise indicated, are from $-\infty$ to ∞ , the asterisk denotes complex conjugate, and $i = \sqrt{-1}$. Also from the autocorrelation theorem,

$$E\{x(u)x^*(v)\} = \int S(\tau) e^{i2\pi(u-v)\tau} d\tau. \quad (A-4.6)$$

Substituting into Eq. (A-4.5),

$$\begin{aligned} E\{C_p(f_{k-j})\} &= \iiint S(\tau) w(u - \frac{L_p}{2}) w^*(v - \frac{L_p}{2}) e^{-i2\pi(u-v)(f_{k-j}-\tau)} du dv d\tau \\ &= \int S(\tau) |W(f_{k-j}-\tau)|^2 d\tau \\ &= \int S(f_{k-j}-\tau) |W(\tau)|^2 d\tau, \end{aligned} \quad (A-4.7)$$

where $W(\tau)$ is the Fourier transform of the data window $w(t)$. ($W(\tau)$ is also referred to as the spectral window.) If we assume that the width of $W(\tau)$ is such that S is approximately constant in a neighborhood of f_{k-j} of that width, then we can make the approximation

$$E\{C_p(f_{k-j})\} \approx S(f_{k-j}) \int |W(\tau)|^2 d\tau. \quad (A-4.8)$$

Further assuming that S is approximately constant over frequencies from f_{k-K} to f_{k+K} , we have from Eq. (A-4.4),

$$E\{\hat{C}(f_k)\} \approx S(f_k) \left[\int |W(\tau)|^2 d\tau \right] \left[\sum_{j=-K}^K a_j \right]. \quad (A-4.9)$$

Turning now to the computation of the variance of $\hat{C}(f_k)$, we can expand in familiar fashion to get

$$\text{Var}\{\hat{C}(f_k)\} = E\{\hat{C}(f_k)^2\} - E^2\{\hat{C}(f_k)\} \quad . \quad (\text{A-4.10})$$

Letting

$$\bar{C}_p(f_k) = \sum_{j=-K}^K a_j C_p(f_{k-j}) \quad ,$$

we can expand Eq. (A-4.10) further to yield

$$\begin{aligned} \text{Var}\{\hat{C}(f_k)\} &= \frac{1}{p^2} \sum_{p=1}^P \text{Var}\{\bar{C}_p(f_k)\} \\ &+ \frac{1}{p^2} \sum_{p \neq q} \left[E\{\bar{C}_p(f_k) \bar{C}_q(f_k)\} - E\{\bar{C}_p(f_k)\} E\{\bar{C}_q(f_k)\} \right] \quad . \quad (\text{A-4.11}) \end{aligned}$$

Note that if the random process x is stationary, then

$$\text{Var}\{\bar{C}_p(f_k)\} = \text{Var}\{\bar{C}_q(f_k)\}$$

for all p and q . Similarly,

$$E\{\bar{C}_p(f_k)\} = E\{\bar{C}_q(f_k)\}$$

for all p and q . Also note that for all p and q such that the corresponding segments of the windowed time function do not overlap

$$E\{\bar{C}_p(f_k) \bar{C}_q(f_k)\} = E\{\bar{C}_p(f_k)\} E\{\bar{C}_q(f_k)\} \quad ,$$

since $\bar{C}_p(f_k)$ and $\bar{C}_q(f_k)$ are independent for this case. Combining all of the above to simplify Eq. (A-4.11) we have

$$\text{Var}\{\hat{C}(f_k)\} = \frac{1}{P} \text{Var}\{\bar{C}_1(f_k)\} + \frac{2(P-1)}{P^2} E\{\bar{C}_1(f_k)\bar{C}_2(f_k)\} - E\{\bar{C}_1(f_k)\} E\{\bar{C}_2(f_k)\} . \quad (\text{A-4.12})$$

(For fractional overlaps less than or equal to 50%, there are $2(P-1)$ pairs of segments that overlap in Eq. (A-4.11)

In order to evaluate Eq. (A-4.12) we will first compute the variance of $\bar{C}_1(f_k)$:

$$\begin{aligned} \text{Var}\{\bar{C}_1(f_k)\} &= \sum_{j=-K}^K \sum_{\ell=-K}^K a_j a_{\ell} E\{C_1(f_{k-j}) C_1(f_{k-\ell})\} \\ &\quad - \left[\sum_{j=-K}^K a_j E\{C_1(f_{k-j})\} \right]^2 . \end{aligned} \quad (\text{A-4.13})$$

We have already computed $E\{C_1(f_{k-j})\}$ in Eq. (A-4.8). Using essentially similar techniques, we can show

$$\begin{aligned} E\{C_1(f_{k-j}) C_1(f_{k-\ell})\} &= \iint S(\mu) S(\tau) \\ &\quad \times \left[|W(f_{k-j} - \mu)|^2 |W(f_{k-\ell} - \tau)|^2 \right. \\ &\quad + W(f_{k-j} - \mu) W^*(f_{k-j} + \tau) W(f_{k-\ell} + \mu) W^*(f_{k-\ell} - \tau) \\ &\quad \left. + W(f_{k-j} - \mu) W^*(f_{k-j} - \tau) W(f_{k-\ell} - \tau) W^*(f_{k-\ell} - \mu) \right] d\mu d\tau . \quad (\text{A-4.14}) \end{aligned}$$

Now assuming that the width of W is small in comparison with f_{k-j} and $f_{k-\ell}$, we can neglect the second term in Eq. (A-4.14) since the windows will not overlap.

$$E\{C_1(f_{k-j})C_1(f_{k-\ell})\} \approx \iint S(\mu)S(\tau) |W(f_{k-j}-\mu)|^2 |W(f_{k-\ell}-\tau)|^2 d\mu d\tau \\ + \left| \int S(\mu)W(f_{k-j}-\mu)W^*(f_{k-\ell}-\mu) d\mu \right|^2 . \quad (A-4.15)$$

Let $\eta = f_{k-j} - \mu$ and $\sigma_{j,\ell} = f_{k-j} - f_{k-\ell}$. Then, again using techniques already demonstrated,

$$\int S(\mu) W(f_{k-j}-\mu) W^*(f_{k-\ell}-\mu) d\mu = - \int S(f_{k-j}-\eta) W(\eta) W^*(\eta+\sigma_{j,\ell}) d\eta \\ \approx - S(f_k) \int W(\eta) W^*(\eta+\sigma_{j,\ell}) d\eta \quad (A-4.16)$$

Substituting back into Eq. (A-4.15), we can obtain

$$E\{C_1(f_{k-j}) C_1(f_{k-\ell})\} \approx S^2(f_k) \left[\left(\int |W(\tau)|^2 d\tau \right)^2 \right. \\ \left. + \left| \int W(\tau) W^*(\tau+\sigma_{j,\ell}) d\tau \right|^2 \right] . \quad (A-4.17)$$

Also necessary in the computation of $\text{Var } \hat{C}(f_k)$ is

$$E\{\bar{C}_1(f_k) \bar{C}_2(f_k)\} = \sum_{j=-K}^K \sum_{\ell=-K}^K a_j a_{\ell} E\{C_1(f_{k-j}) C_2(f_{k-\ell})\} , \quad (A-4.18)$$

where, letting $k-j=n$, $k-l=m$,

$$\begin{aligned} E\{C_1(f_n) C_2(f_m)\} &= \iiint E\{x(u) x^*(v) x(r) x^*(s)\} \\ &\times w(u - \frac{L}{2}) w^*(v - \frac{L}{2}) w(r-L) w^*(s-L) \\ &\times e^{-i2\pi[f_n(u-v) + f_m(r-s)]} du dv dr ds . \end{aligned} \quad (A-4.19)$$

From [Ref. 6], we have

$$\begin{aligned} E\{x(u) x^*(v) x(r) x^*(s)\} &= \iint S(\mu) S(\tau) \\ &\times \left\{ e^{i2\pi[\mu(u-v) + \tau(r-s)]} + e^{i2\pi[\mu(u-r) + \tau(v-s)]} \right. \\ &\left. + e^{i2\pi[\mu(u-s) + \tau(r-v)]} \right\} d\mu d\tau . \end{aligned} \quad (A-4.20)$$

Substituting into Eq. (A-4.19) and integrating with respect to u , v , r , and s yields

$$\begin{aligned} E\{C_1(f_n) C_2(f_m)\} &= \iint S(\mu) S(\tau) \left\{ |W(f_n - \mu)|^2 |W(f_m - \tau)|^2 \right. \\ &+ W(f_n - \mu) W^*(f_n + \tau) W(f_m + \mu) W^*(f_m - \tau) e^{-i\pi(\mu+\tau)L} \\ &\left. + W(f_n - \mu) W^*(f_n - \tau) W(f_m - \tau) W^*(f_m - \mu) e^{-i\pi(\mu-\tau)L} \right\} d\mu d\tau . \end{aligned} \quad (A-4.21)$$

Again, the middle term of Eq. (A-4.21) can be neglected wherever both f_n and f_m are greater than the bandwidth of W . Thus,

$$E\{C_1(f_n) C_2(f_m)\} \approx S^2(f_k) \left[\left(\int |W(\tau)|^2 d\tau \right)^2 + \left| \int W^*(\tau) W(\tau+f_m-f_n) e^{-i\pi L} d\tau \right|^2 \right], \quad (A-4.22)$$

where we have again invoked the assumption that S does not vary significantly over the frequency range from f_{k-K} to f_{k+K} .

Combining Eqs. (A-4.8), (A-4.12), (A-4.13), (A-17), (A-4.18), and (A-4.22) yields

$$\text{Var}\{\hat{C}(f_k)\} \approx \frac{S^2(f_k)}{P} \left[\sum_{j=-K}^K \sum_{\ell=-K}^K a_j a_\ell \times \left\{ \left| \int W(\tau) W^*(\tau+\sigma_{j,\ell}) d\tau \right|^2 + \frac{2(P-1)}{P} \left| \int W(\tau) W^*(\tau+\sigma_{j,\ell}) e^{i\pi\tau L} d\tau \right|^2 \right\} \right]. \quad (A-4.23)$$

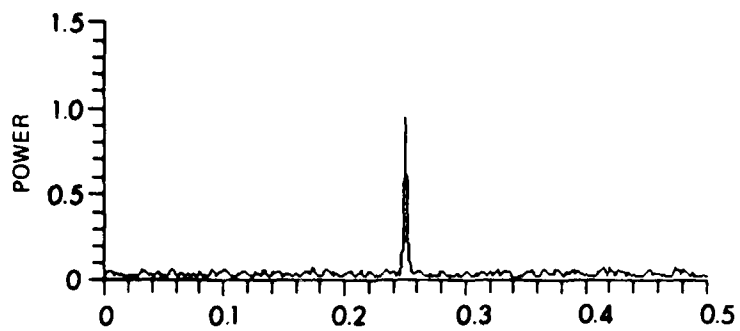
The number of equivalent degrees of freedom of the frequency averaged spectrum can now be found from Eq. (A-4.3) with the aid of Eqs. (A-4.9) and (A-4.23).

APPENDIX 5

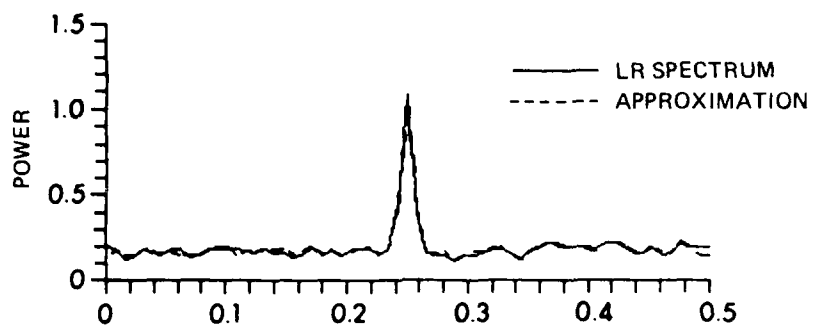
RESOLUTION REDUCTION USING COEFFICIENTS WITH
UNMATCHED EQUIVALENT DEGREES OF FREEDOM

In this appendix we will present examples illustrating the most commonly employed technique for resolution reduction. The procedure is to use frequency averaging with uniform coefficients, using the same number of coefficients as the factor by which resolution is to be reduced. For example, to reduce resolution by a factor of eight, eight uniform coefficients would be used. The difficulty with using this procedure is that neither the spectral window nor the statistics of the frequency averaged spectrum match those of a conventionally obtained spectrum. This can lead to a certain amount of misinterpretation of the results.

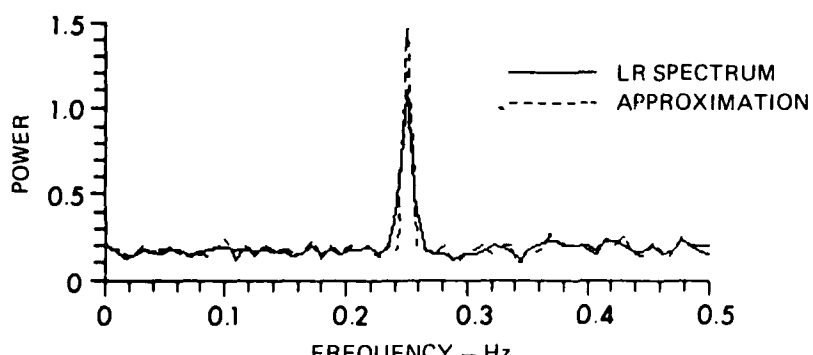
In Figs. 29-34 we show, in the same format used in Chapter IV, examples of spectrum estimates resulting from a 4:1 reduction from a high resolution spectrum. The HSQ coefficients are the same ones used in the previous examples, while four uniform coefficients were used to produce the spectrum shown in the bottom plot of these figures. From the appearance of these plots, we could conjecture that the spectral window associated with the four uniform coefficients is somewhat narrower than the Hanning window used to produce the conventional low resolution estimate. The spectral window comparisons for this type of resolution reduction are shown in Figs. 35-37 for 2:1, 4:1, and 8:1 reduction ratios. An examination of Fig. 36 shows that the window for this 4:1 example is indeed narrower than the Hanning window. Hence, our resolution has not actually decreased by a factor of four, as desired.



HIGH RESOLUTION SPECTRUM



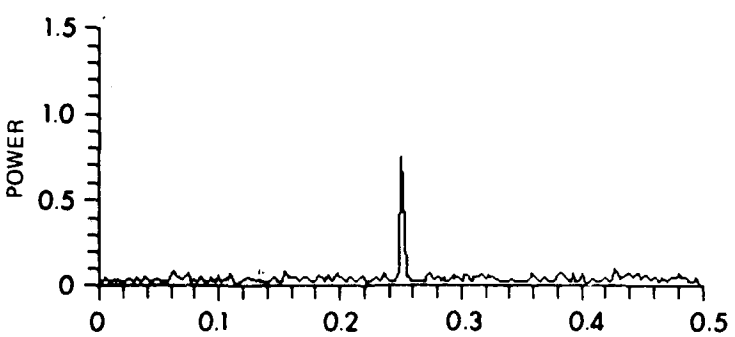
APPROXIMATION OF LR SPECTRUM WITH HSQ COEFFICIENT



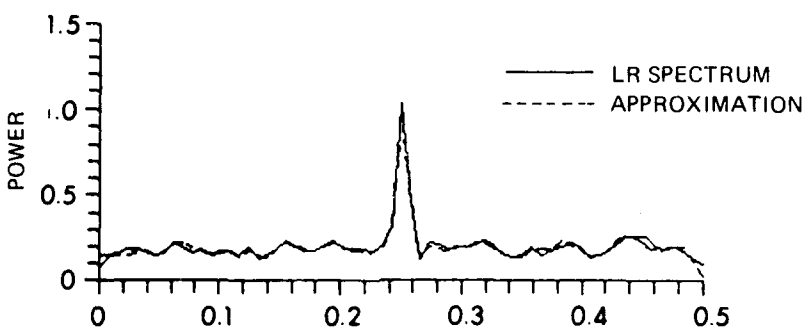
APPROXIMATION OF LR SPECTRUM WITH UNIFORM COEFFICIENT

FIGURE 29
COMPARISON OF POWER SPECTRA
4:1 REDUCTION, $L \times F = 32.000$

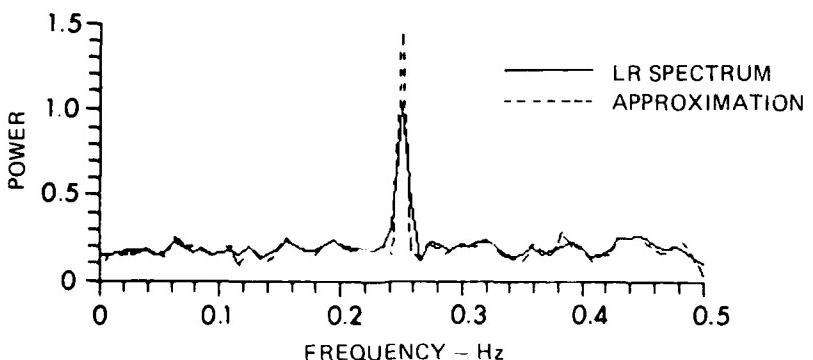
ARL-UT
AS-78-1515
CSP - GA
6-15-81



HIGH RESOLUTION SPECTRUM



APPROXIMATION OF LR SPECTRUM WITH HSQ COEFFICIENT



APPROXIMATION OF LR SPECTRUM WITH UNIFORM COEFFICIENT

FIGURE 30
COMPARISON OF POWER SPECTRA
4:1 REDUCTION, $L \times F = 32.100$

ARL-UT
AS-78-1516
CSP - GA
6-15-81

AD-A100 976

TEXAS UNIV AT AUSTIN APPLIED RESEARCH LABS

F/G 9/4

STATISTICAL CHARACTERISTICS OF POWER SPECTRUM ESTIMATES DERIVED--ETC(U)

N00039-79-C-0306

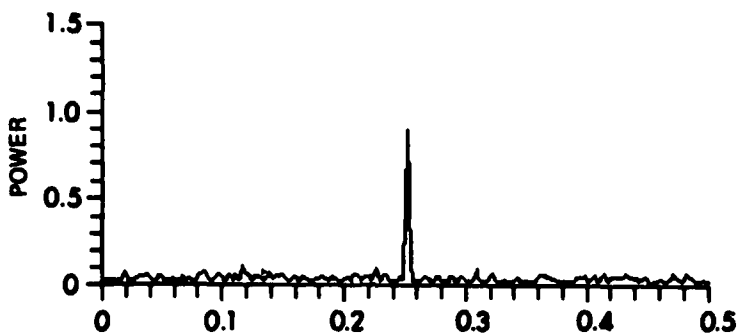
NL

UNCLASSIFIED

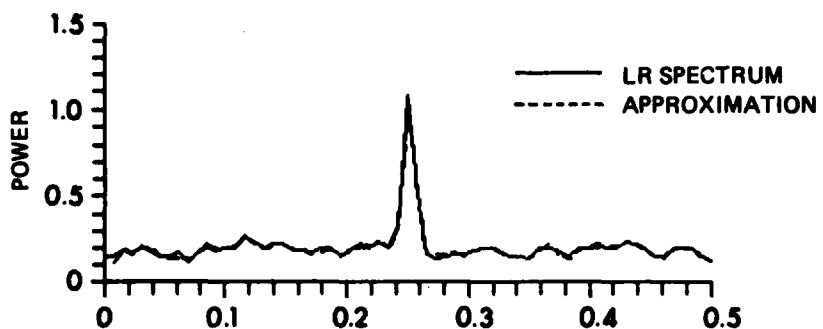
MAY 81 C S PENROD
ARL-TR-81-26

242
2V CDTI

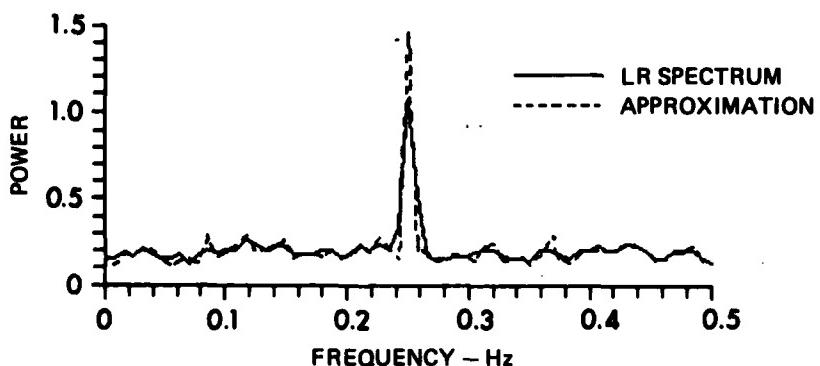
END
DATE PRINTED
7-8-81
DTIC



HIGH RESOLUTION SPECTRUM



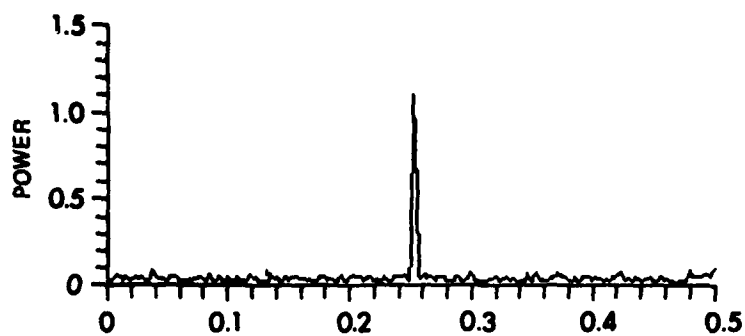
APPROXIMATION OF LR SPECTRUM WITH HSQ COEFFICIENT



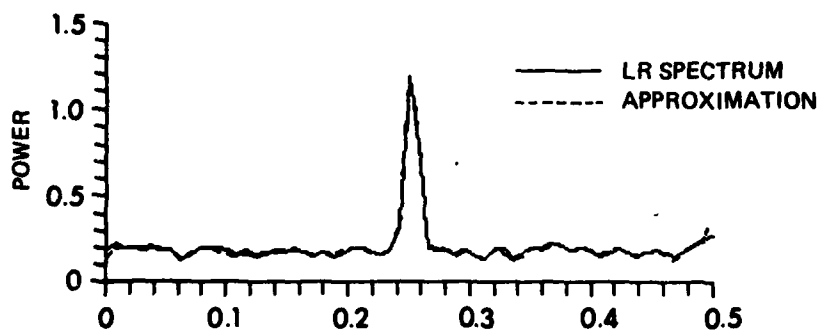
APPROXIMATION OF LR SPECTRUM WITH UNIFORM COEFFICIENT

FIGURE 31
COMPARISON OF POWER SPECTRA
4:1 REDUCTION, $L \times F = 32.200$

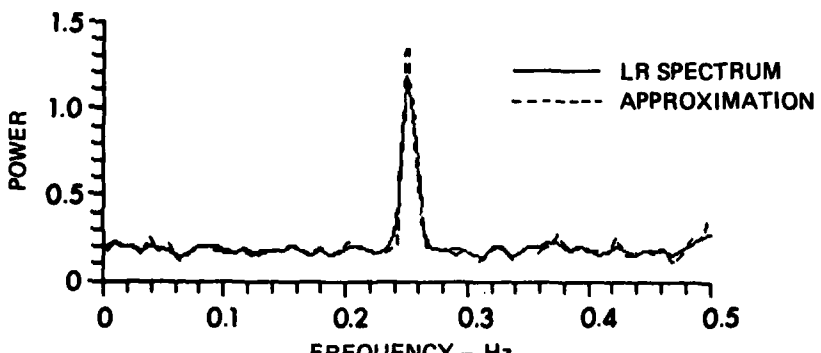
ARL:UT
AS-78-1517
CSP - GA
6-15-81



HIGH RESOLUTION SPECTRUM



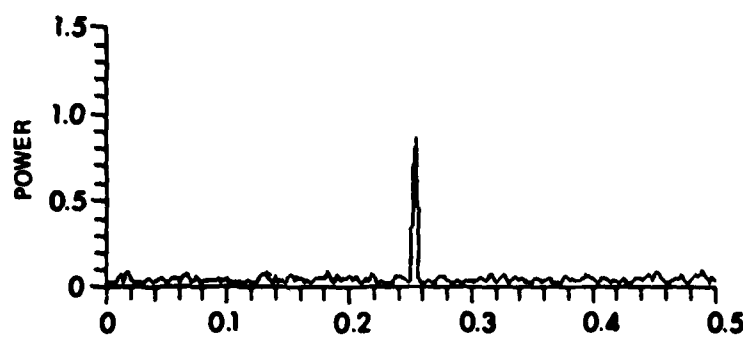
APPROXIMATION OF LR SPECTRUM WITH HSQ COEFFICIENT



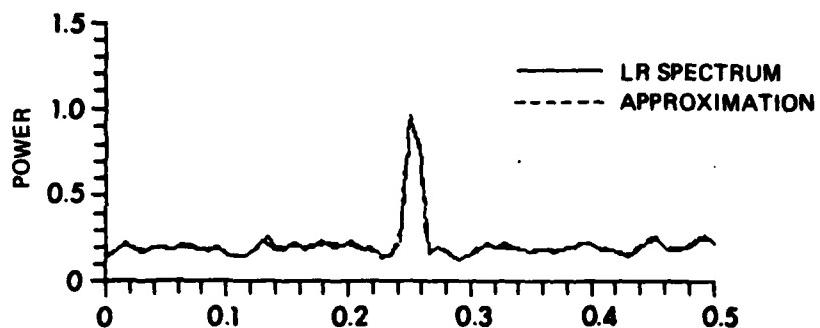
APPROXIMATION OF LR SPECTRUM WITH UNIFORM COEFFICIENT

FIGURE 32
COMPARISON OF POWER SPECTRA
4:1 REDUCTION, $L \times F = 32.300$

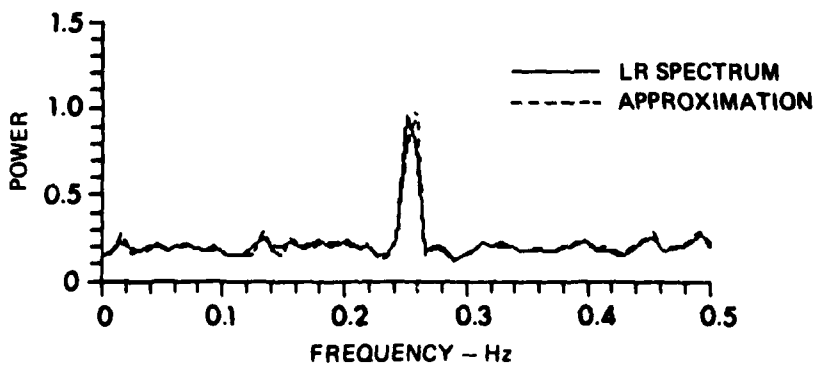
ARL:UT
AS-78-1518
CSP - GA
6-15-81



HIGH RESOLUTION SPECTRUM



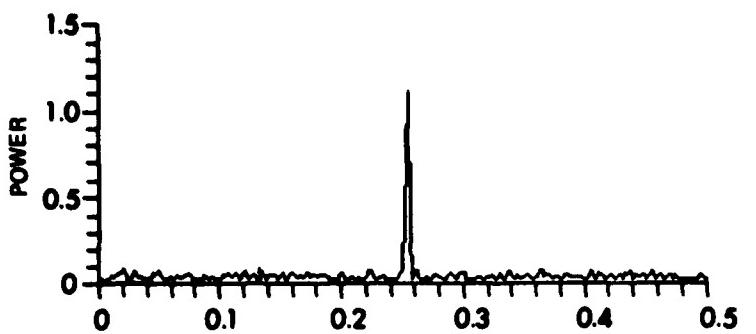
APPROXIMATION OF LR SPECTRUM WITH HSQ COEFFICIENT



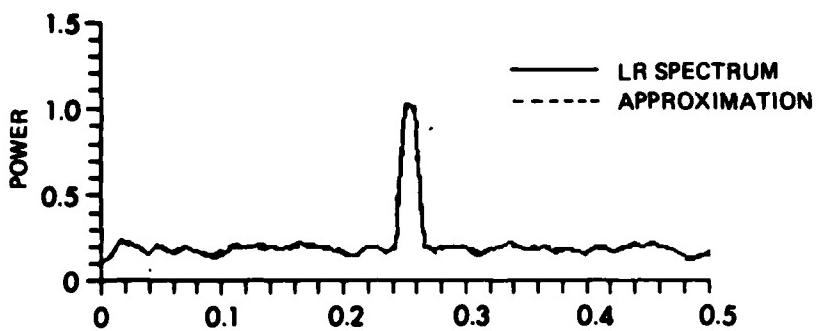
APPROXIMATION OF LR SPECTRUM WITH UNIFORM COEFFICIENT

FIGURE 33
COMPARISON OF POWER SPECTRA
4:1 REDUCTION, $L \times F = 32,400$

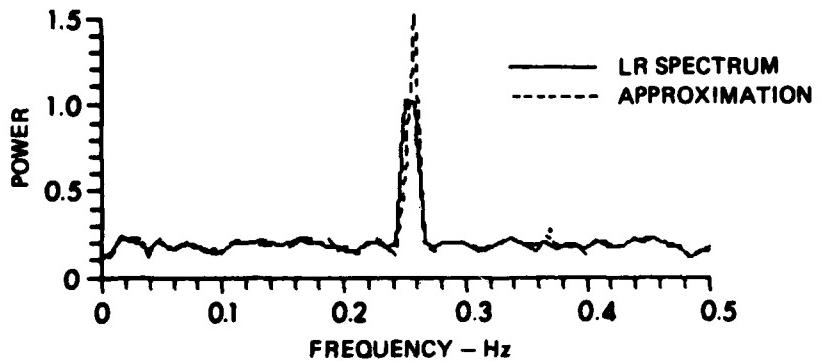
ARL:UT
AS-78-1619
CSP - GA
6-15-81



HIGH RESOLUTION SPECTRUM



APPROXIMATION OF LR SPECTRUM WITH HSQ COEFFICIENT



APPROXIMATION OF LR SPECTRUM WITH UNIFORM COEFFICIENT

FIGURE 34
COMPARISON OF POWER SPECTRA
4:1 REDUCTION, $L \times F = 32.500$

ARL:UT
AS-78-1520
CSP - GA
6-15-81

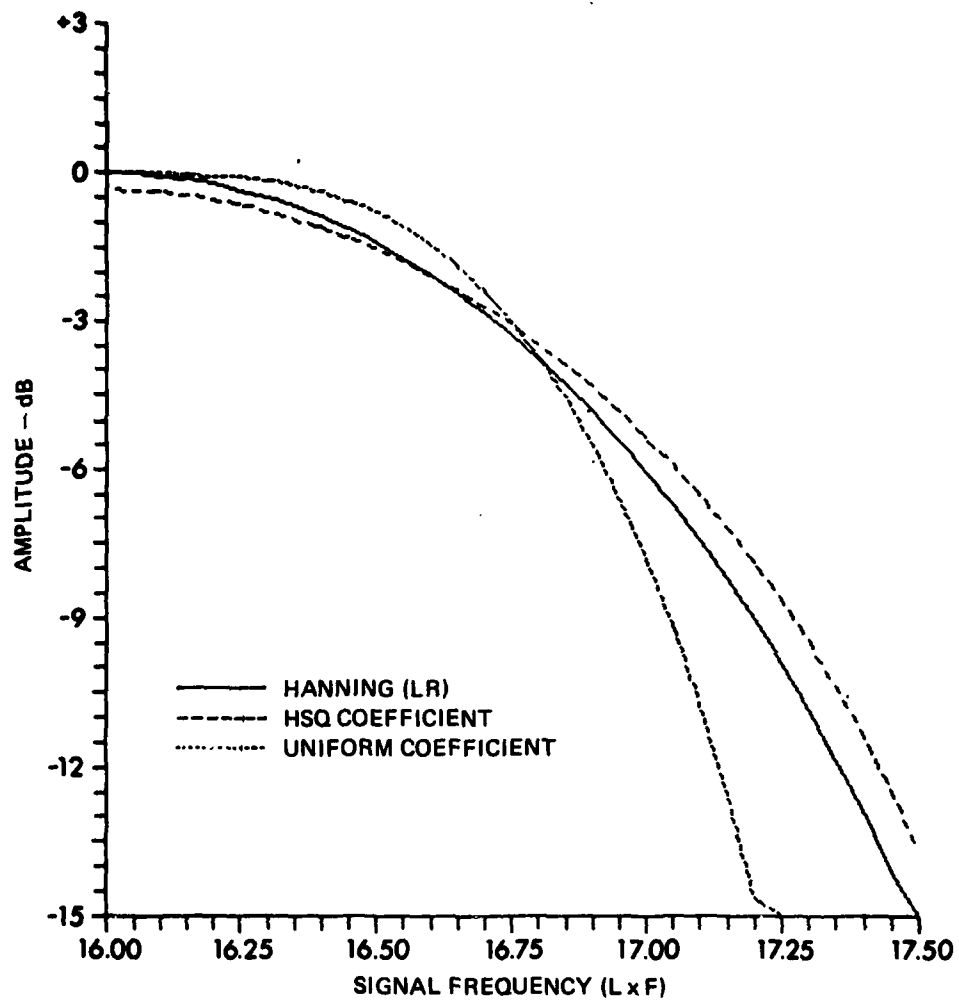


FIGURE 35
SPECTRAL WINDOW COMPARISONS, 2:1 REDUCTION

ARL:UT
AS-78-1521
CSP - GA
6-15-81

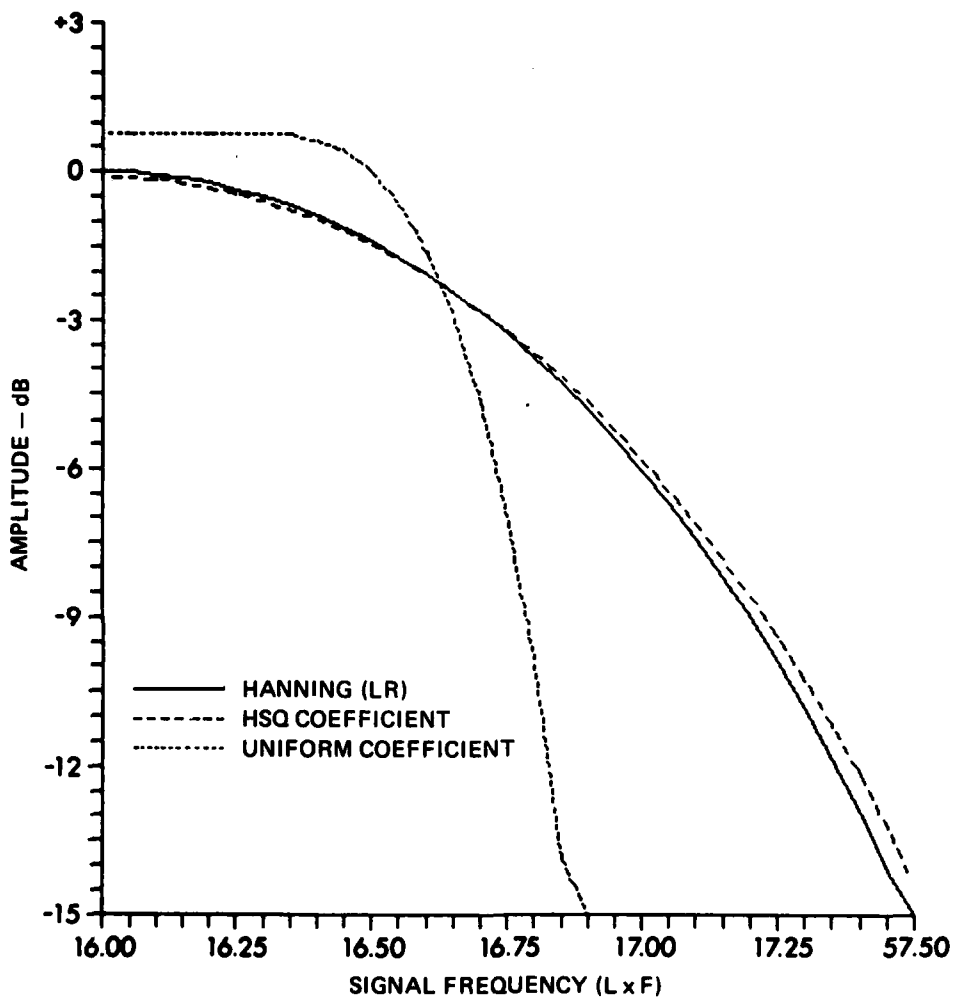


FIGURE 36
SPECTRAL WINDOW COMPARISONS, 4:1 REDUCTION

ARL:UT
AS-78-1522
CSP - GA
6-15-81

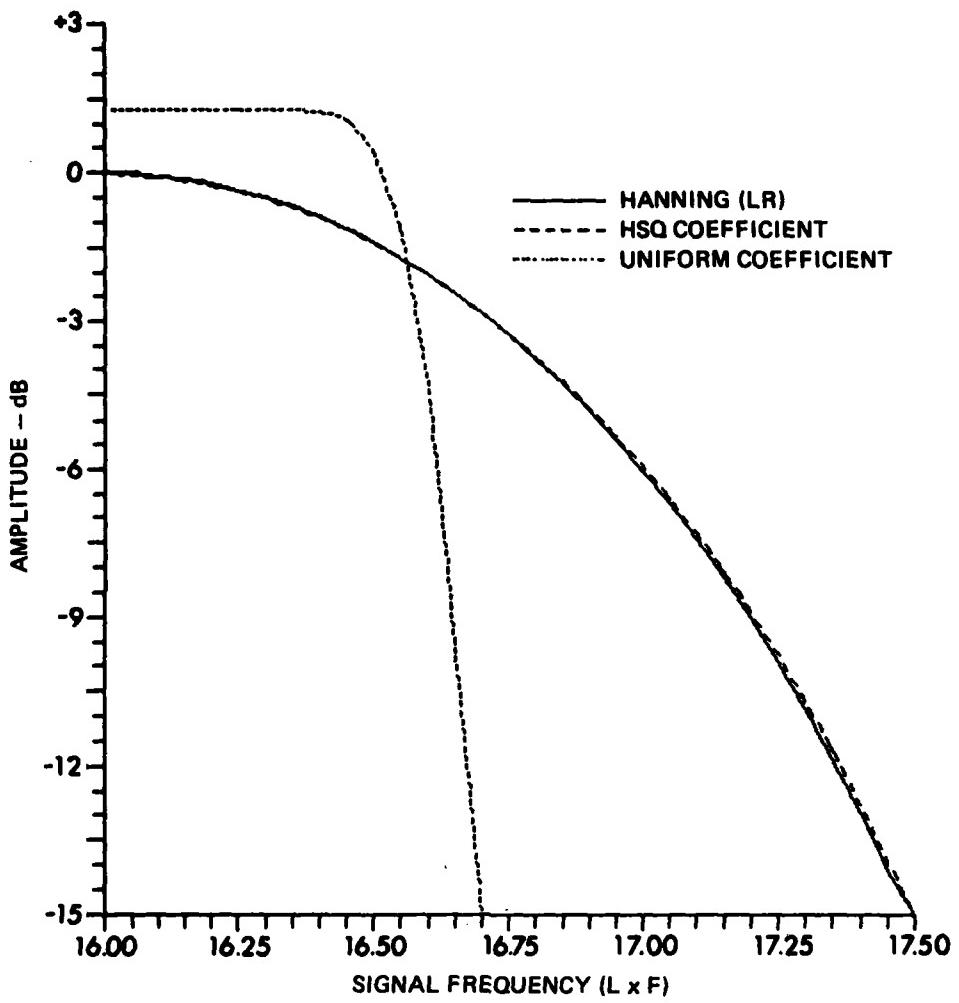


FIGURE 37
SPECTRAL WINDOW COMPARISONS, 8:1 REDUCTION

ARL:UT
AS-78-1523
CSP - GA
6-15-81

Examination of the spectra shown in Figs. 29-34 also suggests that the uniform coefficient frequency averaged estimate lacks the stability of the other low resolution estimates. Computation shows that the conventional low resolution estimate has 89 equivalent degrees of freedom, while the four uniform coefficients produce only 48. This corresponds to an increase in minimum detectable signal level of approximately 1.5 dB. However, over the frequency range of interest, the uniform coefficient window averages approximately 1.2 dB greater than the Hanning window. Hence the net degradation in minimum detectable signal level due to the altered spectral window, neglecting equivalent noise bandwidth changes, is approximately 0.3 dB.

REFERENCES

1. R. B. Blackman and J. W. Tukey, The Measurement of Power Spectra, (Dover Publications, Inc., New York, New York, 1958).
2. G. M. Jenkins and D. G. Watts, Spectral Analysis and Its Applications, (Holden-Day, Inc., San Francisco, California, 1968).
3. G. D. Bergland, "A Guided Tour of the Fast Fourier Transform," IEEE Spectrum, 6, 41-52 (1969).
4. J. W. Cooley, P. A. W. Lewis, and P. D. Welch, "Application of the Fast Fourier Transform to Computation of Fourier Integrals, Fourier Series, and Convolution Integrals," IEEE Trans. Audio Electroacoustics, AU-15, (2), 79-84 (1967).
5. P. I. Richards, "Computing Reliable Power Spectra," IEEE Spectrum, 4, 83-90 (1967).
6. A. H. Nuttall, "Spectral Estimation by Means of Overlapped Fast Fourier Transform Processing of Windowed Data," NUSC Technical Report No. 4169 (Naval Underwater Systems Center) Newport Laboratory, Newport, Rhode Island, 13 October 1971.

DISTRIBUTION LIST FOR
ARL-TR-81-26
UNDER CONTRACT N00039-79-C-0306
UNCLASSIFIED

Copy No.

Commander
Naval Electronic Systems Command
Department of the Navy
Washington, DC 20360
1 Attn: PME-124
2 - 6 PME-124/30
7 PME-124/40
8 PME-124/60
9 PME-124TA

Assistant Director of the Navy (RE&S)
Washington, DC 20301
10 Attn: G. A. Cann

Chief of Naval Operations
Department of the Navy
Washington, DC 20350
11 Attn: OP-095
12 OP-951
13 OP-952
14 OP-094
15 OP-096
16 OP-02
17 OP-03

Chief of Naval Development
Headquarters, Naval Material Command
Washington, DC 20360
18 Attn: MAT-035

Commander
Naval Air Development Center
Department of the Navy
Warminster, PA 18974
19 Attn: Code 250
20 Code 2052
21 Code 2055
22 Code 20P1
23 Code 2604
24 Code 602

Distribution List for ARL-TR-81-26 under Contract N00039-79-C-0306 (Cont'd)

Copy No.

- 25 Chief of Naval Research
Department of the Navy
Arlington, VA 22217
- 26 Commanding Officer
Naval Research Laboratory
Washington, DC 20375
- 27 Attn: Code 8100
- 28 Code 8160
- 29 Commander
Naval Air Systems Command
Department of the Navy
Washington, DC 20360
Attn: Code PMA-264
- 30 Commander
Naval Sea Systems Command
Department of the Navy
Washington, DC 20362
Attn: Code 06R
- 31 Commander
Naval Ocean Systems Center
San Diego, CA 92132
Attn: M. R. Akers
- 32 E. Tunstall
- 33 Commander
Naval Surface Weapons Center
White Oak Laboratory
Silver Springs, MD 20910
- 34 Commander
New London Laboratory
Naval Underwater Systems Center
New London, CT 06320
- 35 Commander
Naval Oceanographic Office
Department of the Navy
Washington, DC 20373
Attn: W. Jobst
- 36 Commanding Officer
Naval Intelligence Support Center
4301 Suitland Road
Washington, DC 20390
Attn: Code 222

Distribution List for ARL-TR-81-26 under Contract N00039-79-C-0306 (Cont'd)

Copy No.

- 38 Commanding Officer
Naval Ocean Research and Development Activity
NSTL Station, MS 39529
- 39 Attn: Code 320
- 40 Code 340
- 41 Code 520
- 42 Code 530
- 43 Defense Advanced Research Projects Agency
1400 Wilson Boulevard
Arlington, VA 22209
Attn: T. Kooij
- 44 ARPA Research Center
Unit 1, Bldg. 301A
NAS Moffett Field, CA 94035
Attn: E. L. Smith
- 45 Superintendent
Naval Postgraduate School
Monterey, CA 93940
- 46 Antisubmarine Warfare Systems Project Office
Department of the Navy
Washington, DC 20360
Attn: PM-4
- 47 - 58 Commanding Officer and Director
Defense Technical Information Center
Cameron Station, Building 5
5010 Duke Street
Alexandria, VA 22314
- 59 Applied Physics Laboratory
The University of Washington
1013 NE Fortieth Street
Seattle, WA 98195
- 60 Bell Telephone Laboratories
2 Whippny Road
Whippny, NJ 07981
- 61 Scripps Institute of Oceanography
The University of California - San Diego
La Jolla, CA 92093
Attn: V. C. Anderson

Distribution List for ARI-TR-81-26 under Contract N00039-79-C-0306 (Cont'd)

Copy No.

- 62 Planning Systems, Inc.
 7900 Westpark Drive
 McLean, VA 22101
 Attn: R. L. Spooner
- 63 Science Applications, Inc.
 8400 Westpark Drive
 McLean, VA 22101
 Attn: J. S. Hanna
- 64 Tetra-Tech, Inc.
 1911 North Fort Myer Drive
 Arlington, VA 22209
 Attn: W. E. Sims
- 65 Tracor, Inc.
 1601 Research Blvd.
 Rockville, MD 20850
 Attn: J. T. Gottwald
- 66 TRW, Inc.
 TRW Defense & Space Systems Group
 Washington Operation
 7600 Colshire Drive
 McLean, VA 22101
 Attn: J. Render
- 67 I. B. Gereben
- 68 Western Electric Company
 P. O. Box 20046
 Greensboro, NC 27420
 Attn: T. Clark
- 69 Woods Hole Oceanographic Institution
 Woods Hole, MA 02543
 Attn: E. E. Hays
- 70 Glen E. Ellis, ARL:UT
- 71 Marshall E. Frazer, ARL:UT
- 72 Kenneth E. Hawker, ARL:UT
- 73 Stephen K. Mitchell, ARL:UT
- 74 Clark S. Penrod, ARL:UT
- 75 Jack A. Shooter, ARL:UT

Distribution List for ARL-TR-81-26 under Contract N00039-79-C-0306 (Cont'd)

Copy No.

76 Library, ARL:UT
77 - 88 Reserve, ARL:UT